TU WIEN

DIPLOMA THESIS

Robust CSI feedback for high user velocity

Institute of Telecommunications of Vienna University of Technology

Laura Portolés Colón

11/18/2014

TECHNISCHE UNIVERSITÄT WIEN
Vienna University of Technology

institute of telecommunications

Abstract

The significant growth of mobile communications usage and the development of new applications that require a wide information flow in the past few years have been the primordial motivations in the investigation of the new mobile communications standard, LTE (*Long Term Evolution*). Release 8 was concluded for the 3GPP (*Third Generation Partnership Project*) in 2008. Significantly higher transmission rates than with the previous technologies has been achieved, up to 326.5 Mbit/s in downlink and up to 86.5 Mbit/s in uplink transmissions due to several improvements that have been introduced on different parts of the communication system.

The work realised in this thesis consist of improving the communications in high velocity scenarios where the channel characteristics deteriorate significantly by means of weak temporal correlation between channel realizations and large latency in the feedback reporting from the UE (*User Equipment*) to the base station (eNodeB). For these reasons this thesis is performed with the downlink link level LTE simulator, available at the Institute of Telecommunications of Vienna University of Technology. The focus of the work is on estimating the feedback parameters, necessary for link adaptation, in high velocity scenarios.

Previously, link adaptation has been optimized for scenarios at low velocity where zero uplink delay can be assumed to obtain sufficiently accurate results. For that reason the CSI (*Channel State Information*) calculation, which is performed in the receiver, is based on instantaneous channel knowledge. As a result of the increasing velocity the performance at the mobile user decreases drastically, because the CSI provided to the base station and utilized for selection of the transmission parameters is very outdated, due to a non-negligible delay in the feedback path. Specifically the CSI consist of three feedback indicators, whose objective is maximizing all the possible gains that OFDM (*Orthogonal Frequency Division Multiplexing*) and MIMO (*Multiple-Input Multiple-Output*) offer, enhancing the channel efficiency while maintaining the BLER (*Block Error Ratio*) below a certain bound, typically fixed to 10% in wireless communications. These three indicators are, CQI (*Channel Quality Indicator*), RI (*Rank Indicator*) and PMI (*Precoding Matrix Indicator*). At high velocity the estimation of these indicators is not accurate enough whether their calculation is exclusively based on the current channel information. Precisely for that reason in this thesis new feedback algorithms that take into account the channel statistics are implemented.

The final objectives of these robust algorithms are the improvement of the channel performance by means of increased throughput and reduced BLER measured in the receiver.

Acknowledgements

I am very glad to have performed this thesis at the Institute of Telecommunications of Vienna University of Technology. I would like to express my gratitude in first place to Prof. Markus Rupp (Vienna University) to allow me to take part in the LTE research group, and in second place to Stefan Schwarz (Vienna University) that has continuously supervised my work leading me to find new solutions to develop in the LTE Vienna simulator. Furthermore, I would like to thank Paloma Garcia (Zaragoza University) for her suggestions and advice from Spain.

There are many other important people that have been present in my life during these last months that I have spent in Vienna. Perhaps they were not with me personally, however, from the distance they have always supported and encouraged me with my studies. The most important are my parents, Inma and Santiago, my sister Cristina and Jaime. Without their backup I could have never lived this unique experience.

Table of Contents

List of Figures

List of tables

List of abbreviations

3GPP	Third Generation Partnership Project
AMC	Adaptative Modulation and Coding
ARQ	Automatic Repeat reQest
AWGN	Additive White Gaussian Noise
BICM	Bit Interleaved Code Modulation
BLER	Block Error Ratio
CB	Code Block
CC	Chase Combining
CLSM	Closed Loop Spatial Multiplexing
CP	Cyclic Prefix
CQI	Channel Quality Indicator
CRC	Cyclic Redundancy Check
CSI	Channel State Information
CW	Codeword
EPC	Evolved Packet Core
ERC	Effective Code Rate
E-UTRAN	Evolved Universal Terrestrial Radio Access Network
EWMA	Exponentially Weighted Moving Average
FDD	Frequency Division Duplex
FFT	Fast Fourier Transform
GPRS	General Packet Radio Services
GSM	Global System for Mobile communications
HARQ	Hybrid Automatic Repeat reQuest
HSPA	High Speed Packet Access
ICI	Inter Carrier Interference
IFFT	Inverse Fast Fourier Transform
IMT	International Mobile Telecommunications
IP	Internet Protocol
IR	Incremental Redundancy
ISI	Inter Symbol Interference
ITU	International Telecommunication Union
LMMSE	Linear Minimum Mean Squared Error
LTE	Long Term Evolution
LTE	Long Term Evolution
LTE-A	Long Term Evolution Advanced
MAC	Medium Access Control
MCS	Modulation and Code Schemes
MIESM	Mutual Information Based Exponential SNR Mapping

MIMO	Multiple-Input Multiple-Output
MME	Mobility Management Entity
OFDMA	Orthogonal Frequency Division Multiplexing Access
OLSM	Open Loop Spatial Multiplexing
PAPR	Peak-to-Average Power Ratio
PCCC	Parallel Concatenated Convolutional Code
P-GW	Packet data network Gateway
PHY	Physical Layer
PMI	Precoding Matrix Indicator
QAM	Quadrature Amplitude Modulation
RB	Resource Block
RE	Resource Element
RI	Rank Indicator
RLC	Radio Link Control
RRM	Radio Resource Management
SAE	System Architecture Evolution
SC-FDMA	Single Carrier Frequency Division Multiplexing Access
S-GW	Serving Gateway
SINR	Signal to Interference plus Noise Ratio
SISO	Single-Input Single-Output
SNR	Signal to Noise Ratio
SSD	Soft Sphere Decoding
STBC	Space-Time Block Code
TB	Transport Block
TDMA	Time Division Multiplexing Access
TTI	Transmission Time Interval
TU	Typical Urban
UE	User Equipment
UMTS	Universal Mobile Telecommunication System
WCDMA	Wideband Code Division Multiplexing Access
ZF	Zero Forcing

1. INTRODUCTION AND MOTIVATION

After about twenty years of practically uninterrupted growth of mobile communications, not only referred to voice but also video streaming and other real time applications that require wideband data flow, a new generation of wireless communication, 3G, has been exhaustively investigated in the past few years. LTE (*Long Term Evolution*), is a new standard, concluded for the 3GPP (*Third Generation Partnership Project*) in 2008 (Release 8), which can be considered the first step in the evolution that will culminate with LTE-Advanced (4G). The most relevant aspects about LTE are that for the first time IP (*Internet Protocol*) is supported for all its services, voice included, and the peak rates reached in the radio interface are in the range of 100Mbit/s to 1Gbit/s, considerably higher than with previous technologies, namely, GSM (*Global System for Mobile communications*) or UMTS (*Universal Mobile Communication System*) Release 7. Furthermore it was expected that with the appearance of LTE the capacity achieved by the mobile users would not be substantially penalized because of the velocity, however this goal is not achieved.

The high transmission rates can be achieved by virtue of the new physical layer architecture implemented, together with other improvements. OFDMA (*Orthogonal Frequency Division Multiplexing Access*) modulation scheme is utilized in DL (*Downlink*) transmissions whose advantage with respect to the previous modulation schemes used is that it converts the wide-band frequency selective channel into a set of many flat fading subchannels. The fact that the signal is divided into flat fading channels has some advantages, for instance that optimum receivers can be implemented with reasonable complexity in contrast to WCDMA (*Wideband Code Division Multiplexing Access*) utilized in the previous communication standard. Furthermore it allows scheduling in the frequency domain, trying to assign physical resources to users with optimum channel conditions. In addition, OFDMA facilitates its implementation in MIMO (*Multiple-Input Multiple-Output*) that consists in the use of several antennas for transmission and reception. MIMO allows exploiting multi-user diversity as well as several different gains that it offers (diversity gain, multiplexing gain and array gain), promising an important transmission rate improvement without increasing bandwidth or transmit power. On the contrary, SC-FDMA (*Single-Carrier Frequency Division Multiplexing Access*) is utilized in the uplink due to its low PAPR (*Peak-to-Average Power Ratio*).

The main objectives of the LTE standard are efficiency increase, cost reduction, extension and improvement of the already provided services and a greater integration with the existent protocols. In normal conditions these objectives are fulfilled, however when the scenario deteriorates, i.e high velocity user scenarios, the performance decreases drastically.

The algorithms as well as the results comparison are conducted with the LTE Vienna Simulators, available at the institute of Telecommunications (Vienna University of Technology). In that context the simulations are performed in the downlink link level where the data is transmitted by a base station (eNodeB) through the channel and is received by several mobile users.

In low velocity scenarios the channel temporal correlation is large and zero UL (*Uplink*) delay can be assumed, nevertheless, when the velocity increases significantly (above 50km/h) the channel behaviour deteriorates drastically. There is negligible temporal correlation between different channel realizations and as a result the received signal suffers from strong fluctuations. Furthermore, the uplink delay can be very large compared to the channel coherence time.

LTE implements link adaption, whose objective is to improve the link efficiency, by maximizing all the possible gains that OFDM and MIMO offer, while maintaining the BLER (*Block Error Ratio*) below a bound, typically fixed to 10% in wireless communications. For that purpose the base station requires updated CSI, which should be provided by user feedback. This CSI consist of three indicators, namely, CQI (*Channel Quality Indicator*) that represents the highest modulation and coding scheme that the channel supports to achieve the BLER target at the first HARQ (*Hybrid Automatic Repeat reQuest*) transmission; RI (*Rank Indicator*), which signals the recommended transmission rank, that is, the number of spatial streams (layers) that can be used in downlink transmissions and finally the PMI (*Precoding Matrix Indicator*) that indicates which of the predefined precoding matrices maximizes the channel performance. When employing CSI feedback based on instantaneous channel conditions at high velocity, the latency in the feedback reporting leads to numerous transmissions errors. This occurs because the information received at the base station is outdated and the selected transmission parameters are not appropriate for the new channel conditions experienced during transmission. In order to deal with this problem in this thesis new feedback algorithms that are based on statistical channel information are implemented.

Chapter 2 explains the advantages and the most important aspects of the LTE physical layer architecture, which implements an OFDM modulation scheme, the frame structure and feedback modelling. Some relevant parameters that are considered in wireless communications are also detailed and finally, the characteristics and architecture of the downlink link level simulator employed to perform this thesis are explained.

In chapter 3 and 4 the results obtained through simulating the new proposed algorithms are shown. When it comes to interpreting the results presented, the fact that the HARQ process could not be applied should be taken into account. In chapter 3 the objective is to accomplish the BLER boundary of 10% while trying to achieve the maximum throughput. In chapter 4 the objective is also to fulfil the BLER target but in

this case without being concerned about the BLER values, which are above 10% in most of the cases. In practice, with the use of HARQ transmissions, an important BLER downturn is expected, as explained in [1]. In both chapters the estimation of the three feedback indicators named above in high velocity scenarios is studied using a flat fading channel and one user. The feedback indicators estimation should not be based exclusively on instantaneous channel knowledge due to its fast variations and the large feedback latency. With the purpose of studying the CQI calculation the most simple antenna configuration is used, i.e., SISO (*Single-Input Single-Output*). Different methods that consider the statistics of several variables, for instance, the SINR (*Signal to Interference plus Noise Ratio*) at the receiver or the selected CQI, are compared. In some cases, long-term average filters are applied and in other cases the throughput or BLER expected are estimated for each possible modulation and coding scheme, selecting the most suitable indicator depending on the final objective. With the purpose of studying the RI and PMI it is necessary to use more complex antenna configurations that require spatial preprocessing. The simplest antenna configuration with more than one layer is employed, that is, 2x2 MIMO that incorporates two transmit antennas and two receiver antennas. The disadvantage of the PMI adaptation at very high velocity is studied and a simple algorithm to select the most appropriate RI is implemented. Finally, also in both chapters, the implemented methods that achieve the best performance are evaluated over time and frequency selective channels with multiple users.

Some algorithms have been developed before to adapt the transmission rate at high speed, two specific examples are available in references [2] and [3]; however, since it is not possible to know the distance between the base station and the user in the context of this thesis, their implementation has been inviable.

Finally, the main conclusions are synthetized and the possible future research lines are commented.

2. LONG TERM EVOLUTION

2.1 Long Term Evolution description

2.1.1 Mobile communications evolution

The first generation cellular system was based on analog transmissions, being able to support voice with some supplementary services. During the 1980s digital communications started to be investigated and a second-generation of mobile communication standard started to be developed. The first standard in Europe was GSM, based on TDMA (*Time Division Multiple Access*). After some years, GPRS (*General Packet Radio Services*) was standardized (often referred to as 2.5G), which enhanced the network and added more features.

The work on a third-generation started in 1998 in ITU (*International Telecommunication Union*) when the 3GPP was formed by organizations from different parts of the world. A new standard was developed, UMTS, based on WCDMA and containing all features needed to fulfil the IMT-2000 (*International Mobile Communications 2000*, name for 3G standards) requirements. The voice and video services were circuit-switched while data services were transmitted over both packet-switched and circuit-switched communication methods. The most important addition of radio access features to WCDMA was with HSPA (*High-Speed Downlink Packet Access*) and Enhanced Uplink. The 3G evolution continued and in 2004 the work on the 3GPP LTE started.

The work on IMT-Advanced (4G) commenced in 2008 with the study on LTE-Advanced. The task was to define requirements and investigate technology components. LTE-Advanced is therefore not a new technology; it is an evolutionary step in the continuing development of LTE. Figure 2-1 shows the 3GPP evolution [17].

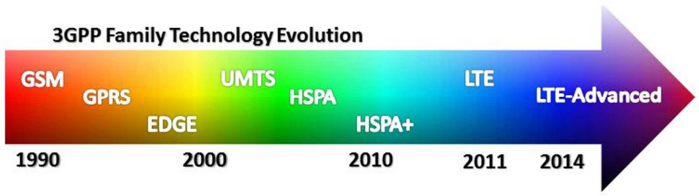

Figure 2-1 3GPP Technology Evolution (referencia)

2.1.2 LTE requirements and characteristics

The main technical objectives accomplished by 3GPP are listed below.

- Significantly increased peak data rate, with instantaneous rate of 100 Mbit/s on the downlink and 50 Mbit/s on the uplink using a 20Mhz system bandwidth
- All the services are packet-switched
- Improved spectrum efficiency by a factor of three to four in downlink and two to three in uplink compared to the previous technology, that allows significant capacity increase.
- Scalable bandwidth of 1.4, 3, 5, 10, 15 and 20 MHz depending on the data rate needed by the user. It provides high market flexibility.
- Assures the maximum capacity for user speed between 0-15 km/h and high performance for speeds up to 120 km/h. Furthermore the connection is maintained up to 350 km/h with capacity degradation.
- Maintains the compatibility with earlier releases and with other systems. It allows co-existence between operators in adjacent bands as well as cross-border.
- Low data transfer latencies, below 5ms for small IP packets in optimal conditions, lower latencies for handover and connection setup time than with previous radio access technologies.
- Simplified architecture, the network side of E-UTRAN is composed only of eNodeBs.
- Large cells with a radius exceeding 120 km can be used because OFDM parameters can be adjusted for different cell sizes.

2.1.3 Network architecture

An additional goal of LTE was the redesign and simplification to an all IP-based system architecture with significant low latency and good scalability.

The LTE core network is named SAE (*System Architecture Evol*ution), which is divided into the EPC (*Evolved Packet Core*) and the E-UTRAN (*Evolved Universal Terrestrial Radio Access Network*). A scheme of this structure is represented in Figure 2-2 [18].

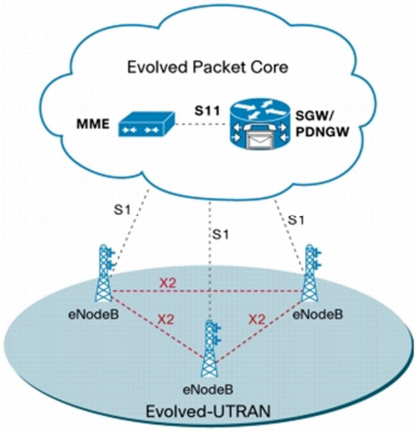

Figure 2-2 Network architecture -LTE/EPC Reference Architecture

The EPC performs numerous functions for idle and active terminals, signaling information related to mobility and security and dealing with the IP data traffic transport between the User Equipment and the external networks. The main difference with respect to the predecessor architectures is that the management layer is removed and now the RRM (*Radio Resource Management*) is developed in the base stations, now called eNodeBs (*Evolved Base Stations*). E-UTRAN is composed of the eNodeBs that perform all radio interface-related functions for terminals in active mode (RRM), i.e. radio resource control, admission control, load balancing and radio mobility control, including handover decisions between other functionalities.

The eNodeBs are connected directly via S1 interfaces to the EPC and also are mutually interconnected via X2 interfaces, providing a much greater level of direct interconnectivity and resulting in a much simpler architecture.

2.1.4 Physical layer

The physical level technologies employed in LTE constitute one of the main differences with respect to the predecessor systems.

LTE Frame structure

OFDM is the modulation scheme utilized in DL, which is a multi-carrier transmission mechanism whose main advantage is that it divides the wide-band frequency selective channel into a set of many flat fading subchannels. OFDM multiplexes several symbols over adjacent subcarriers and afterwards all of them are transmitted simultaneously enabling the separation in the receiver without much complexity.

OFDM employs a set of K adjacent narrowband subcarriers that have the property to be orthogonal as shown in Figure 2-3 [8]. The symbols are modulated with 4, 16 or 64 QAM (*Quadrature Amplitude Modulation*) depending on the selected modulation scheme. Due to its specific structure OFDM allows for low complexity modulator by means of computationally efficient IFFT (*Inverse Fast Fourier Transform*) and demodulator implementation by means of FFT (*Fast Fourier Transform*) respectively.

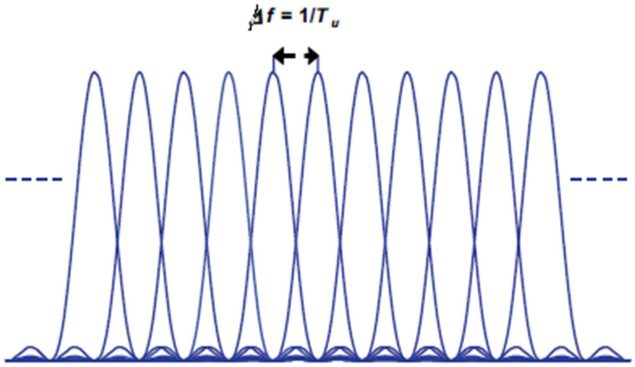

Figure 2-3 OFDM subcarrier spacing

In wireless communications, the channel is usually time-dispersive due to multipath and the orthogonally between subcarriers can be lost leading to ISI (*Inter Symbol Interference*) and ICI (*Inter Carrier Interference*). In order to deal with that problem OFDM uses CP (*Cyclic Prefix*) insertion in the transmission (that consists on the copy of the last part of the OFDM symbol at the beginning) that makes the OFDM signal insensitive to time dispersion as long as the time dispersion does not exceed the length of the cyclic prefix. As a consequence the OFDM symbol rate is reduced.

Table 2-1 OFDM configuration

Configuration		N_{sc}^{RB}	N_{symb}^{DL}	CP Length (μs)
Normal cyclic prefix	$\Delta f = 15\ kHz$	12	7	4.69
Extended cyclic prefix	$\Delta f = 15\ kHz$	12	6	16.67
	$\Delta f = 7.5\ kHz$	12	3	33.33

The frame structure of the FDD (*Frequency Division Duplex*) is depicted in Figure 2.4. In time domain the transmitted signal is organized in radio frames with duration of 10ms. In the same way each radio frame is subdivided into ten subframes with duration 1ms, also called TTI (*Transmission Time Inteval*), and finally those are divided into two slots. In the frequency domain the whole bandwidth is divided into equally-spaced orthogonal subcarriers with scalable bandwidth although the typical subcarrier spacing is 15 kHz. Subcarriers are organized in groups named RB (*Resource Block*), which is the minimum physical resource that can be assigned to one user. For the 15 kHz spacing 12 subcarriers and one slot time duration belong to each RB. Table 2-1 lists the different possible configurations and Figure 2-4 [5] shows the time-frequency grid structure for 15 kHz subcarrier spacing and normal CP length. Each element in this grid is called RE (*Resource Element*) and defines the unit to position the transmitted data.

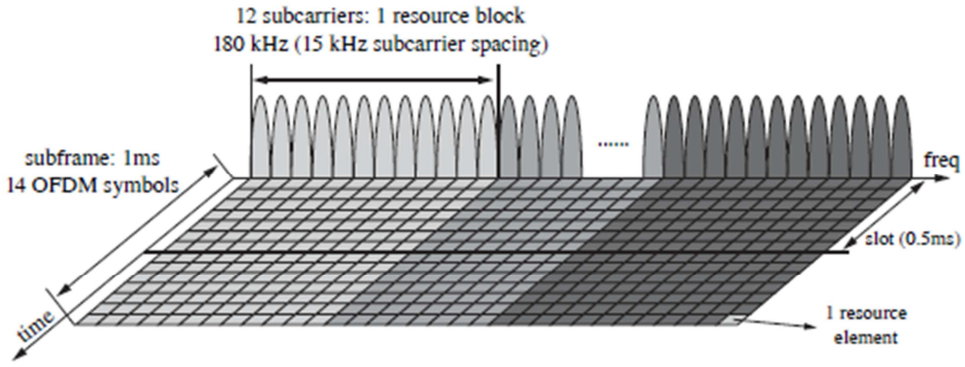

Figure 2-4 LTE time-frequency grid structure (reference)

There are two different training symbols, namely, synchronization signal and reference signal (also called pilot symbols), which are located in specific REs. The reference symbols are used to estimate the frequency domain channel around the REs that they occupy. The density of the reference symbols must be sufficiently high to be able to provide estimates for the entire time-frequency grid in case the radio channel is subjected to strong frequency and/or time selectivity.

Despite these proper features, OFDM has two important drawbacks. The first one is the frequency synchronization sensibility and the second and more important is the large variations in the instantaneous power of the transmitted signal, PAPR, that impairs any multi-carrier transmission. These variations imply reduced power-amplifier efficiency (because they should work in linear regime) and higher power-amplifier cost. Several methods haven been proposed to reduce the power peaks, however most of them imply significant computational complexity and reduced link performance.

This is the main reason for why SC-FDMA is used in Uplink transmissions, because a low PAPR is a crucial factor to be able to work with amplifiers in the non-linear zone in order to achieve high transmission power in the mobile user without signal distortion. As well as in the downlink the transmitted signal is divided into radio frames of 10 ms.

Multi-Antenna techniques

Multi-antenna techniques can be used to achieve improved system performance, including improved system capacity (more users per cell) and improved coverage (possibility for larger cells), as well as improved service provisioning, for example higher per-user data rates. The Release 8 and 9 supports one, two and four transmit antennas (larger number of transmit antennas increase the pilot overhead) while in the receiver there is no limitation. Release 10 can support up to 8 transmit antennas. The different transmit modes that use multi-antenna techniques are detailed in section 2.2.

2.2 LTE feedback modelling

LTE supports AMC in order to adapt the transmission parameters to the current channel conditions based on instantaneous channel knowledge. Additionally when MIMO is used the spatial preprocessing (transmission rank, precoding) is also adaptive trying to maximize the possible MIMO gains. For that purpose the base station requires uploaded CSI, which should be provided by UE feedback. The final aim of this CSI feedback is to maximize the obtainable throughput while maintaining the BLER below a certain threshold, set to 10% for mobile communication systems. LTE requires the calculation of up to 3 different feedback indicators depending on the transmission mode selected. In this chapter the different feedback indicators and transmission modes are explained in detail.

2.2.1 User equipment feedback indicators

- **Rank indicator (RI)**,

  This indicator signals the recommended transmission rank to use, that is, the number of independent data streams that are transmitted simultaneously on the same time and frequency resources. At low Signal to Noise Ratio, SNR, in general is better to implement beamforming while at high SNR a larger throughput can be achieved by spatial multiplexing several parallel data streams. In LTE Rel. 8 and 9 this indicator will range between one and four due to four is the maximum number of transmit antennas specified.

- **Precoding matrix indicator (PMI),**

Indicates which of the precoding matrices defined in codebooks should preferably be used for the downlink transmission in order to maximize the user throughput. The chosen PMI value is associated to the number of transmission layers given by RI. Table 2-2 show the available precoding matrices when the number of transmit antennas is two. In [4] it can be consulted the complete LTE codebook for CSLM transmission mode.

Table 2-2 LTE codebook for CSLM mode and two transmit antennas

Codebook index	Number of layers (v)	
	1	2
0	$\frac{1}{\sqrt{2}}\begin{bmatrix}1\\1\end{bmatrix}$	-
1	$\frac{1}{\sqrt{2}}\begin{bmatrix}1\\-1\end{bmatrix}$	$\frac{1}{2}\begin{bmatrix}1 & 1\\1 & -1\end{bmatrix}$
2	$\frac{1}{\sqrt{2}}\begin{bmatrix}1\\i\end{bmatrix}$	$\frac{1}{2}\begin{bmatrix}1 & 1\\1 & -i\end{bmatrix}$
3	$\frac{1}{\sqrt{2}}\begin{bmatrix}1\\-i\end{bmatrix}$	-

- **Channel-quality indicator (CQI),**

Represents the highest modulation-and-coding scheme that, if used, would achieve the given BLER target at the first HARQ transmission. In wireless communications this target is typically BLER < 0.1. Basically the CQI provides information to the base station about the current quality of the channel realization in terms of a quantized SINR. There are 15 MCSs (*Modulation and Coding Schemes*) specified in table 2-3 (4-bit indicator). The CQI signals for each codeword which one of those MCSs ensures the BLER below the threshold. Each CQI specifies a code rate between 0.08 and 0.92, as well as 4, 16 and 64-QAM modulations. It should be noted that such SINR-to-CQI mapping depends on the type of receiver used. A better receiver would be able to feedback higher CQIs than other simpler receiver in the same channel conditions.

A combination of the RI, PMI, and CQI forms the complete Channel State Information. This combination actually depends directly on the eNodeB configured transmission mode considering that the RI and PMI do not need to be reported unless the terminal is in a spatial multiplexing transmission mode.

Table 2-3 Modulation scheme and effective coding rate for each of the Channel Quality Indicators (CQIs)

CQI Index	Modulation	ERC	Data [bit/symbol]
0	Out of range		
1	4-QAM	0.08	0.15
2	4-QAM	0.12	0.23
3	4-QAM	0.19	0.38
4	4-QAM	0.30	0.60
5	4-QAM	0.44	0.88
6	4-QAM	0.59	1.18
7	16-QAM	0.37	1.48
8	16-QAM	0.48	1.91
9	16-QAM	0.60	2.41
10	64-QAM	0.46	2.73
11	64-QAM	0.55	3.32
12	64-QAM	0.65	3.90
13	64-QAM	0.75	4.52
14	64-QAM	0.85	5.12
15	64-QAM	0.93	5.55

The wireless channel is in general time as well as frequency selective and as a result the most suitable feedback values can vary over consecutive RBs. In transmission, the eNodeB applies the same CQI value to all RBs assigned to the same user. Even though the system is configured to calculate a single CQI value for each RB, the base station would determine an average CQI over the resource blocks assigned to the same user. On the contrary, the base station can apply different PMI to consecutive RBs irrespective of the RBs correspond to the same user or not. Due to these factors a subband CQI and PMI calculation can be highly beneficial in presence of frequency-selective channels when more than one user is being served.

2.2.2 Transmission modes

SISO : Transmission mode 1

This is the simplest antenna configuration. It consists of one transmit base station that utilizes a single transmitter antenna and one receive mobile user that also incorporates one single receiver antenna. Only one stream can be transmitted with single antennas, which is the reason why only the CQI is needed at the base station.

Transmit diversity: Transmission mode 2

Can be applied to any downlink physical channel but is especially useful at transmissions that cannot be adapted to varying channels conditions by means of link adaptation, and thus for which diversity is more important. The Alamouti Space-Time Block Code (STBC) is used to fix the precoding matrix and the number of transmission layers only depends on the number of transmit antennas. As in the previous case, only the CQI indicator feedback is needed.

Open Loop Spatial Multiplexing (OLSM): Transmission mode 3

This mode represents a codebook-based precoding scheme that does not rely on any PMI recommendation from the user and the precoding matrix is also fixed by some standard in order to achieve multiplexing and/or diversity gain. This mode is mostly used in high-mobility scenarios where the latency in the PMI reporting is high and an accurate feedback is difficult to achieve. That is why there is no requirement of signalling the current precoder used for the downlink transmission. On the other hand the transmission rank can be adapted and this requires RI and CQI feedback information.

Since only the RI and CQI are available, OLSM incorporates Cyclic Delay Diversity. This basically shifts the transmit signal in time direction and transmit these two signals over different transmit antennas. Since the shifts are inserted cyclically there is no additional Inter-Symbol Interference. The diversity is increased without additional receiver complexity because with that process the number of resolvable propagation paths is higher.

Closed Loop Spatial Multiplexing (CLSM): Transmission mode 4

This is also a codebook-based precoding scheme where the optimum precoding matrix index is reported by the user, in addition to the RI and CQI. This mode can give gain in scenarios where the channel does not vary rapidly and there is a low latency in the PMI reporting, thus accurate feedback information can be achieved. The precoding matrix is selected from a codebook where the available precoding matrices are indexed. In order to simplify signalling only the index is sent. Table 2-2 lists the possible precoder matrices for 2 antennas. For the four antenna case the codebook includes up to 64 precoding matrices.

2.2.3 SISO feedback calculation

As commented above no spatial preprocessing is needed in this case. For that reason the feedback information needed at the base station for a properly transmission is only the CQI. This choice is based on a mapping between post equalization SINR and CQI for a SISO AWGN channel. The SINR-to-CQI mapping table was obtained by simulating the BLER performance for all CQI values. The SINR values in the table are equal to the AWGN SNRs at 10 % BLER. Once the SINR is estimated at the receiver, it is compared to the SINR values in the tables and the maximum CQI that allows transmission without exceeding 10 % BLER is selected. SINR values below the SNR point obtained from the curve simulated with CQI 1 are mapped to a CQI equal to 20, which means out of range and whose correspondent spectral efficiency is zero.

Different CQI granularities are supported to give the scheduler the opportunity to schedule users located in favourable resources, so as to maximize the overall cell throughput.

2.2.4 MIMO CSLM feedback calculation

In MIMO systems the feedback for link adaptation comprises the three indicators explained at the beginning of this chapter. If not all these values are used the optimization with respect to the indicator not employed is omitted and a corresponding predefined value is used. CQI and PMI can be wideband (if an average feedback value is calculated over the whole bandwidth) or subband estimated (the available bandwidth is divided into subbands and different CQI and PMI values are calculated for each one), and depending on the channel characteristics a specific CQI and PMI granularity is optimum.

In order to reduce the complexity of the optimization problems in the CSI calculation described in section 10.4.2 of [5] and in [6] a new sequential optimization is implemented in the downlink level simulator, studied in detail in [7]. A short explanation of this estimation is explained below.

The total system bandwidth, consisting of R REs, is divided into S subbands. The set of REs belonging to subband s is denoted R_s. Furthermore a mapping is defined, $\rho : \{1, \dots, \mathrm{R}\} \rightarrow \{1, \dots \mathrm{S}\}$ which assigns a RE r to the corresponding subband s.

The first step consist of finding the optimum subband precoder, W_s. The precoder for subband s is defined as follows,

$$W_s = W^{(1)} \cdot W_s^{(2)} \tag{2.1}$$

The rank dependant precoder codebook, defined in [4], is denoted by $\mathcal{W}^{(V)}$. In equation 2.1 $W^{(1)}$ denotes the wideband precoder and $W_s^{(2)}$ the subband precoder for subband s.

With the aim to find the preferred subband precoders the spectral efficiency of each RE r, denoted I_r, is computed for all combinations of precoders (W_s) and transmission ranks (V). This spectral efficiency corresponds to the post-equalization mutual information, which is calculated by means of the BICM (*Bit Interleaved Code Modulation*) capacity with respect to all subband precoders. The BICM capacity is modulation alphabet dependent and utilizes a function $f(SNR)$ whose envelope represents the maximum efficiency over all modulation alphabets. Figure 2-5 represents this function [5],

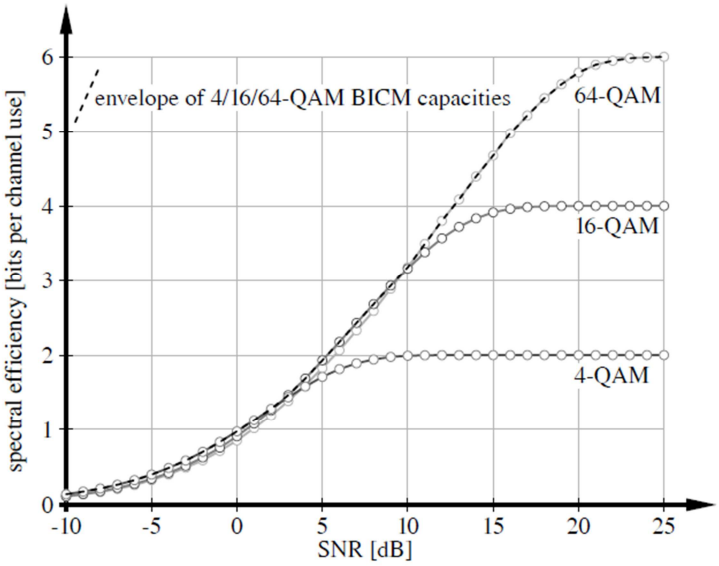

Figure 2-5 BICM capacity of 4, 16 and 64-QAM modulation [4]

$$f(SNR) = \max_{a \in A} f_a(SNR) \tag{2.2}$$

In this equation, $f_a(SNR)$ denotes the BICM capacity with respect to all defined modulation alphabets $a \in A = \{A_4, A_{16}, A_{64}\}$, which are respectively 4, 16 or 64-QAM. The estimated spectral efficiency of RE r is,

$$I_r(W_s, V) = \sum_{v=1}^{V} f(SINR_{r,v}(W_s)) \tag{2.3}$$

Where V denotes the transmission rank and W_s the subband precoder. The post-equalization $SINR_{r,v}$ calculation is required (the most expensive step because of the need to compute matrix inversions in order to calculate the receive equalizer filter) according to,

$$SINR_{r,v}(W_s) = \frac{P_v \cdot |K_r[v,v]|^2}{\sum_{i \neq v} P_i \cdot |K_r[v,i]|^2 + \sigma_n^2 \sum_i |F_r[v,i]|^2} \tag{2.4}$$

$$r \in \{1, \dots, R\}, \quad v \in \{1, \dots, V\}$$

In equation 2.4 P_v denotes the transmit power on layer v, F_r the equalizer on RE r, P_i is the interference caused by the other transmission layers, σ_n^2 the noise power spectral density and $K_r[v,i]$ refers to the element in the vth row and ith column of matrix Kr, which depend on the precoder and is defined as,

$$K_r = F_r H_r W_s \qquad s = \rho(r), \quad H_r \in \mathbb{C}^{N_R \times N_T} \tag{2.5}$$

where $\mathrm{H_r}$ is the channel matrix. Then the sum spectral efficiency for each subband is maximized in order to choose subband precoders.

$$I_s(W_s, V) = \sum_{r \in R_s} I_r(W_s, V) \tag{2.6}$$

$$\widehat{W}_s^{(2)}\left(W^{(1)}, V\right) = \underset{W_s^{(2)} \in W_2^{(V)}}{\operatorname{argmax}} I_s(W_s, V) \tag{2.7}$$

These optimum subband precoders $\widehat{W}_s^{(2)}$ for each possible transmission rank, V, and wideband, S, are stored, as well as the spectral efficiency, I_s, whose sum over all subbands for each rank is maximized.

$$I(W_s, V) = \sum_{s=1}^{S} I_s(W_s, V) \tag{2.8}$$

As a result, a first approximation to the preferred rank V is found.

$$\hat{V} = \underset{V \leq V_{max}}{\operatorname{argmax}} I\left(\widehat{W}_s(V), V\right), \qquad \widehat{W}_s(V) = \widehat{W}^{(1)}(V)\widehat{W}_s^{(2)}(V) \tag{2.9}$$

Afterwards, the RI is obtained by maximization of the sum efficiency over layers. Since the previous mutual information estimation is not always accurate enough, the sum efficiency over layers is calculated for $\hat{V}$ and $\hat{V} - 1$. For each of these ranks and each layer the equivalent AWGN channels are estimated. Then, an average SINR is estimated for each subband, values that are mapped to CQIs. Each CQI represents a certain spectral efficiency, E_S, that is summed over layers (CQI parameters are listed in section 2.2.1) and finally the maximization of the sum efficiency over ranks $\hat{V}$ and $\hat{V} - 1$ results in the final RI

$$\left[\hat{V}, \{\widehat{W}_s\}_S, \{\hat{m}_s\}_S\right] = \underset{L, W^{(1)}, W_s^{(2)}, m_s}{\operatorname{argmax}} \sum_{s=1}^{S} \sum_{c=1}^{C_L} E_s^c(W_s, m_s[c]) \tag{2.10}$$

Subject to: $V \leq V_{max}$

$$W^{(1)} \epsilon \mathcal{W}_1^{(V)}$$

$$W_s^{(2)} \epsilon \mathcal{W}_2^{(V)}$$

$$m_s \epsilon \mathcal{M}^{C_V \times 1}$$

The value $\hat{m}_s[c]$ denotes the optimal AMC scheme $m \in \mathcal{M}$ for subband s and codeword c. In the case of SU-SISO just CQIs are provided per codeword. The preferred RI equals $\hat{V}$ and the constraint on the number of transmission layers $V \leq V_{max}$ follows from the rank of the channel matrices

$$V_{max} = \min_{r \in \{1,\ldots,R\}} rank(H_r) \tag{2.11}$$

Detailed information about LTE and CQI, PMI and RI calculation can be found in [4], [5] and [6].

2.3 High velocity consequences

Rayleigh fading is the statistical model used to simulate the propagation effect. It can be applied in wireless communications when there is no dominant propagation along the line of sight between the transmitter and the receiver. In a Rayleigh faded channel the normalized autocorrelation function is expressed by means of the Jake's model [10]

$$R(\tau) = J_0(2\pi f_d \tau) \tag{2.12}$$

Where J_0 denotes a zero order Bessel function of the first kind, f_d refers to the maximum Doppler shift and τ is the delay. The product of the maximum Doppler shift and the delay is known as Normalized Doppler frequency, $\overline{f_d}$,

$$\overline{f_d} = f_d \tau \qquad \text{with} \qquad f_d = v\frac{f_0}{c} \tag{2.13}$$

Where v refers to the user velocity, f_0 is the carrier frequency and c represents the speed of light. In Figure 2-6 the behaviour of the normalized autocorrelation function over normalized Doppler frequency is represented. It can be observed how the

temporal correlation decreases, reaching cero at 0.38 normalized Doppler frequency. Then the correlation fluctuates, never taking values above 0.4.

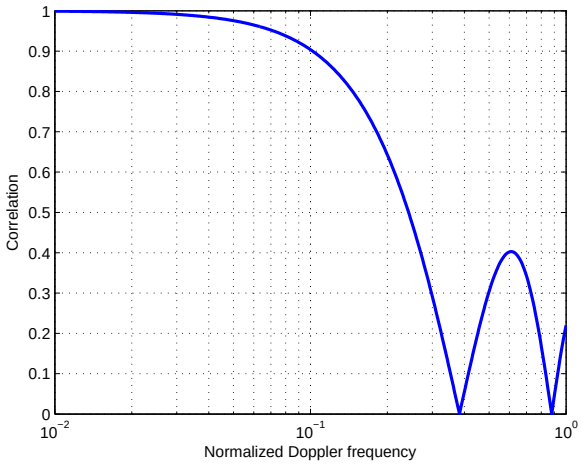

Figure 2-6 Temporal correlation in a Rayleigh fading channel

Other relevant parameter at high velocity is the channel coherence time, which can be substantially short compared to the uplink delay in high velocity scenarios. The channel coherence time is the time duration over which the channel impulse response is considered to be not varying. According to Clarke's model ,[11] and [19], the expression that defines the channel coherence time can be expressed as,

$$T_C = \sqrt{\frac{9}{16\pi\, f_d^2}} \simeq \frac{0.423}{f_d} \qquad (2.14)$$

where f_d denotes again the maximum Doppler shift. From this expression it can be seen how an $\overline{f_d}$ increase, caused by a velocity increase, results in a lower channel coherence time. When these expressions are evaluated at 2.1 MHz carrier frequency and 100 km/h (velocity used with SISO antenna configuration) the maximum Doppler frequency is 194.56 Hz and the channel coherence time is 2.2ms. At 250 km/h (velocity used for MIMO simulations) the maximum Doppler frequency is 486.45 Hz and the channel coherence time is 0.87ms. Considering that the uplink delay used in the simulations is 10ms, the CSI received at the base station can be assumed completely outdated information and virtually uncorrelated with respect to the current channel conditions.

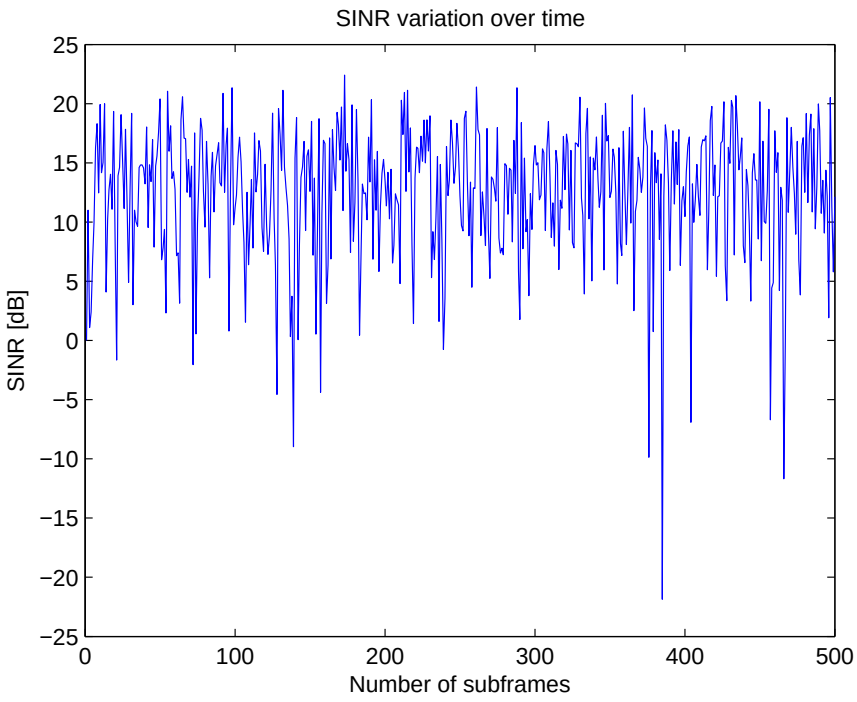

Figure 2-7 SINR variation between consecutive subframes at high velocity

In Figure 2-7 the post-equalization SINR calculated in the receiver is represented over time. Strong and fast fluctuations in the channel conditions are the cause of these SINR variations, which can be more than 20dB between consecutive subframes.

The user performance obtained with the same simulation parameters in terms of throughput and BLER can be seen in Figure 2-8. The results show an important loss in throughput, with respect to the results obtained by applying the original algorithm with zero UL delay, as well as a BLER exceeding the 0.1 target.

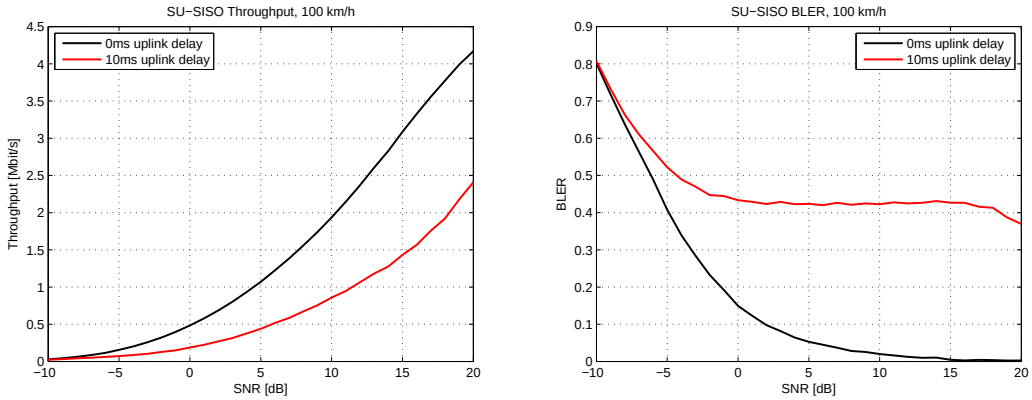

Figure 2-8 Performance loss due to the feedback delay

2.4 Vienna LTE simulators

In the past few years reproducible research has been an important objective in the field of signal processing, and even more important as the simulated systems become more and more complex. This is the case for wireless communication systems. Researchers often demand to access the original source code to reproduce and verify the results presented. The Vienna LTE simulators, as an open source software plataform, are a very important tool to carry out these verifications.

The Vienna LTE simulator is a standard-compliant open-source Matlab-based simulation platform, which supports link and system level simulations and that implements UMTS LTE.

> *Link level simulations* are used to investigate e.g. channel estimation, tracking, prediction and synchronization algorithms, MIMO gains, AMC *(Adaptive Modulation and Coding*), feedback techniques, receiver structures and channel modelling.
>
> *System level simulations* are used to investigate network issues, such as resource allocation and scheduling, multi-user handling, mobility management, admission control, interference management and network planning optimization. A network consists of multiple eNodeBs that cover a specific area in which many mobile terminals are located or moving around.

The complete structure of these simulators is explained in [12] and [13]. In these papers it is also explained how link and system level are connected, because the former serves as a reference for designing the latter. Moreover, the wide capabilities of the simulator can be observed through some examples of its application.

To be able to investigate different feedback algorithms implemented during this thesis, all the simulations are performed in the downlink link level simulator.

The link level simulator consists of three building blocks, namely, transmitter, channel model and receiver that are represented in Figure 2-9 [12].

- *Transmitter*. Based on UE feedback the scheduler assigns the available RBs to UEs, setting the appropriate MCS, transmission mode and precoding/number of spatial layers.

- *Channel model*. This simulator supports block and fast-fading channels. The available channel models are AWGN, flat Rayleigh fading, Power Delay Profile-based such as ITU Pedestrian A/B or ITU Vehicular A/B, TU (Typical Urban) and Winner II among others.

- *Receiver*. The simulator supports ZF (*Zero Forcing*), LMMSE (*Linear Minimum Mean Squared Error*) and SSD (*Soft Sphere Decoding*) as detection algorithms. After detection the channel is estimated and the feedback indicators are calculated.

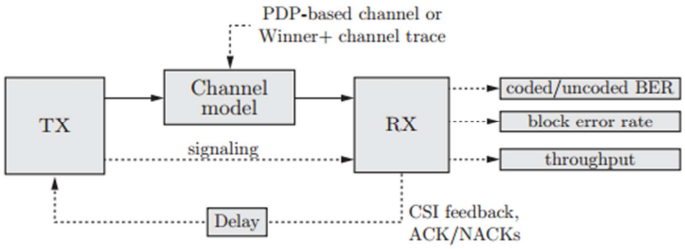

Figure 2-9 Downlink link level simulator architecture

In a downlink transmission, the data is generated in the transmitter, sent through the channel model and detected at the receiver. The channel model introduces signal distortions, such as time- and frequency-selective fading. . This data contains signalling information, i.e. coding, HARQ, scheduling and precoding parameters that are assumed to be error-free due to the low coding rates and low order modulation utilized.

The uplink signalling and feedback transmission are also assumed error-free. The only considered distortion is a delay in the feedback path.

2.4.1 Main simulation parameters

In table 2-4 the main simulation parameters that remains constant during all the simulations can be found.

Table 2-4 Constant simulation parameters

Carrier frequency	2.1 GHz
System bandwidth	1.4 MHz
Subcarrier spacing	15 kHz
Receiver	Zero forcing (ZF)
Channel model	Block fading
Channel estimation	Perfect
Number of eNodeBs	1

For both the development of the methods that estimate the CQI and the comparison of them over SNR, it is employed a scenario with unfavorable characteristics. The simulation parameters appear in table 2-5.

Table 2-5 Simulation parameters utilized do develop the methods to estimate the CQI

Transmission mode	1
Channel model	Flat Rayleigh
UL delay	10 ms
Number of users	1

In order to compare the methods that estimate the CQI over the normalized Doppler frequency the following simulation parameters in table 2-6 are used.

Table 2-6 Simulation parameters utilized to compare the CQI methods over $\bar{f}_d$

Transmission mode	1
Channel model	Flat Rayleigh correlated
UL delay	1 ms
Number of users	1
User velocity	Variable (0-300 km/h)

The sections where the PMI and RI are investigated utilize the simulation parameters written in table 2-7.

Table 2-7 Simulation parameters in order to study PMI and RI

Transmission mode	4
Channel model	Flat Rayleigh
UL delay	10 ms
Number of users	1
Rx antenna correlation	0.5 (Kronecker model)

Finally when the methods are evaluated using a frequency selective channel the parameters in table 2-8 are applied.

Table 2-8 Simulation parameters to evaluate the methods in a frequency selective channel

Transmission mode	4
Channel model	Flat Rayleigh correlated
UL delay	1 ms
Number of users	6
User velocity	Variable (0-300 km/h)

3. FEEDBACK ALGORITHMS TO IMPROVE THE USER THROUGHPUT

In this chapter, the new algorithms designed to improve the throughput in high mobility scenarios are presented. These algorithms are implemented without being concerned about the BLER resuslts, which are above 10% in most of the cases. It is expected that in practice, applying the HARQ process, the BLER target will be achieved.

3.1 Study of the CQI

3.1.1 SINR Long-term average

The first step in this method consists of changing the SINR mapping table to obtain the maximum possible throughput. With the feedback deactivated, the throughput curves for each CQI are simulated over SNR and applying the parameters in table 2-5. Then a new mapping table is created by selecting the SNR points that achieve the maximum throughput for each CQI. Figure 3-1 represents the maximum throughput achieved for each CQI separately.

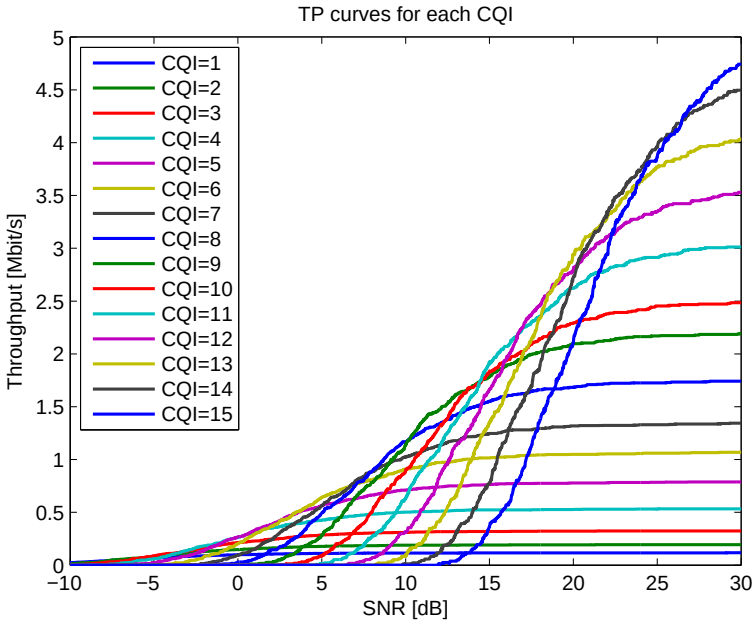

Figure 3-1Maximum throughput curves for CQI 1-15

In addition, this method estimates an SINR long-term average at the receiver. Several methods that calculate the average of some parameters over time have been studied

before, two examples can be found in [14] and [15]. The expression employed in this method is the Exponentially Weighted Moving Average (EWMA), a type of infinite impulse response filter that applies weighting factors which decrease exponentially. The weighting for each older datum decreases exponentially, never reaching zero.

$$\overline{SINR}_n = \left(1 - \frac{1}{\beta}\right)\overline{SINR}_{n-1} + \left(\frac{1}{\beta}\right)SINR_n \tag{3.1}$$

In that expression the parameter β defines the weight factors applied to the instantaneous $SINR_n$ and the previous averaged $\overline{SINR}_{n-1}$. The larger is beta, the smaller weight factor is applied to the current SINR value. Beta value is chosen by simulations, and in this case where there is no temporal correlation a value beta equal to 10 is employed. Smaller beta values result in lower throughput while larger beta values result in the same performance.

3.1.2 Maximum throughput expected

This method consists of trying to learn the CQI statistics, which are a-priori unknown to the user. Based on these CQI statistics, the expected throughput is estimated and maximized with respect to the CQI. An scheduling method that maximizes the throughput with adjustable fairness is detailed in [16]. Similar expressions are applied here to calculate the maximum throughput expected.

At each realization an instantaneous approximation of the CQI probability mass function (pmf) is estimated with the CQI calculated for the current channel conditions, denoted CQI_n. This CQI_n value has been calculated through mapping the instantaneous $SINR_n$.

$$p_n(i) = \frac{1}{R}\sum_{r=1}^{R} 1\left[CQI_n(r) = i\right] \qquad i \epsilon 1, \dots, N_{AMC} \tag{3.2}$$

In this expression i as well as R denote the number of available modulation and coding schemes. The only non-zero value in this vector, $p_n(i)$, is located in the position whose index is equal to the CQI_n selected by the algorithm. Then this vector is averaged over time employing the same type of exponential averaging filter as in the previous method, i.e., EWMA.

$$\hat{p}_n = \left(1 - \frac{1}{\beta}\right)\hat{p}_{n-1} + \left(\frac{1}{\beta}\right)p_n \tag{3.3}$$

$\hat{p}_n$ indicates the probability that a given CQI is instantaneously optimal. The beta value is again chosen by simulations, selecting as in the previous method beta equal to 10.

After that the expected throughput is estimated for each CQI "i", as the product of the spectral efficiency of CQI "i" and the probability that the channel supports this CQI, i.e., the sum of the probabilities of all CQIs larger than or equal to "i"

$$T_{exp}(CQI_i) = efficiency(CQI_i) \cdot \sum_{cqi \geq CQI_i} \hat{p}_n(cqi) \qquad i \in 1, \dots, N_{AMC} \qquad (3.4)$$

Finally the CQI with highest expected throughput is selected to be fed back over the uplink channel.

3.1.3 Conditional CQI probability

This method estimates the CQI that maximizes the throughput based on the knowledge of the probability of the UE to choose a specific CQI when the previous CQI selected is known.

For that purpose, the probability of a specific CQI to be selected depending on the previous CQI employed is needed. These probabilities are calculated in first place storing in a squared matrix, of length the number of modulation and coding schemes, the number of times that a specific CQI is selected. The matrix indexes where the instantaneous CQI, denoted CQI_n , is stored at each realization are given in the first dimension by the CQI value calculated in the previous realization, denoted CQI_{n-1} , and in the second dimension by the current CQI_n. Figure 3-2 is an example of the data matrix at 100km/h, 10dB SNR, 10ms uplink delay and 1000 simulated subframes. For a specific previous CQI, it can be seen how many times each CQI has been chosen at the next realization.

Once these data has been stored in a matrix, the probability vectors for each CQI_{n-1} (previous CQI) are estimated. Each value of this matrix is divided by the sum of the number of CQIs stored in the row that it occupies. The result is a matrix that consists of N_{AMC} probability vectors, which indicate the probability of a specific CQI to be selected depending on the previous CQI.

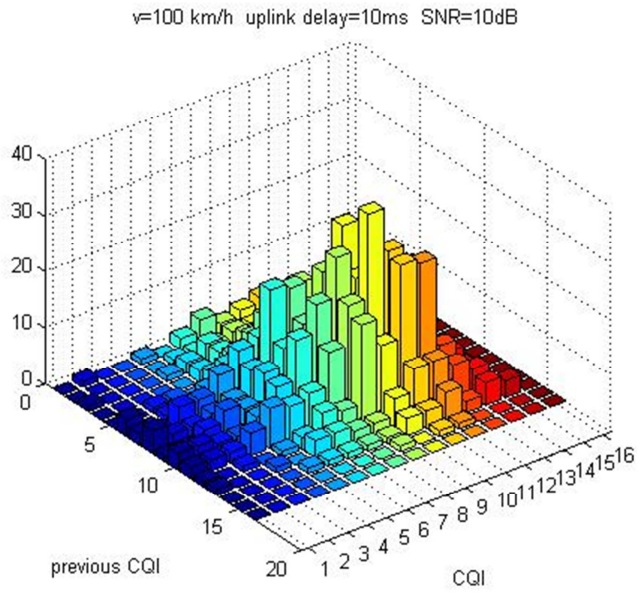

Figure 3-2 CQI dependant on the previous CQI

Once this probability vectors are available the method can be applied. At each realization one instantaneous CQI, CQI_n , is estimated through SINR_n mapping. Moreover, the CQI selected in the previous realization, CQI_{n-1}, is also known because it has been stored. This CQI_{n-1} is used to index the row of the matrix previously calculated, obtaining a probability vector denoted as $p_{CQI_{n-1}}$.

Finally the throughput expected is calculated using the same expression as in the previous method (equation 3.4), employing as $\hat{p}_n$ the probability vector indexed by CQI_{n-1}, that is, $p_{CQI_{n-1}}$. Finally the CQI that maximizes the expression is fed back over the uplink channel.

The main disadvantage of this method is that it is necessary to store the CQIs selected over time to calculate the correspondent probability vectors before applying the method. Moreover, this data matrix has to be calculated for each specific speed, SNR point and uplink delay, resulting in an excessive computational cost.

3.1.4 SINR variation

With the goal of simplifying this method, a new procedure is implemented based on the same idea. It basically consists of storing in a vector, whose length increases with the number of simulated subframes, the SINR variation between consecutive subframes over time. At each realization the probability distribution of the stored SINR variation values up to that time is fitted by a *t location-scale* distribution function, which is denoted as $P(\Delta SINR)$. The *t location-scale* distribution is useful for modelling data with heavier tails (more prone to outliers) than the normal distribution.

Figure 3-3 represents an example of the SINR variation distribution setting 10dB SNR, 10ms uplink delay, 1000 simulated subframes and at 100km/h and 50km/h,. The lower the velocity, the narrower and picked the distribution becomes because the SINR variations are less pronounced.

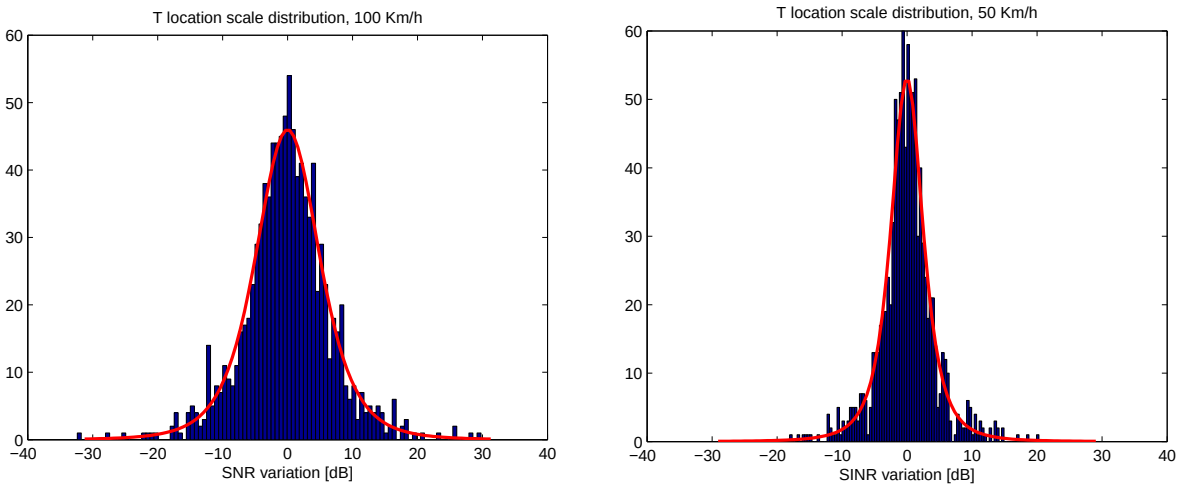

Figure 3-3 T location-scale distribution function

Then the difference between the instantaneous SINR, denoted as $SINR_n$, and the necessary SINR to select each different CQI, $SINR(CQI_i)$, is estimated. $SINR(CQI_i)$ is a vector whose values correspond to the values in the mapping table.

$$\Delta SINR_n(i) = SINR_n - SINR(CQI_i) \qquad i \in 1, \dots, N_{AMC} \tag{3.5}$$

As a result, a vector of necessary SINR variations, $\Delta SINR_n(i)$, of length the number of modulation schemes, N_{AMC}, is obtained.

After that, and for each possible CQI, the probability than the SINR variations will be above the values calculated in equation 3.5 are estimated. These probabilities are computed using the complementary cumulative distribution function (ccdf), which corresponds to the upper probability tail of the *t location-scale* distribution function for each $\Delta SINR_n(i)$ value

$$\hat{p}_n(i) = P\big(\Delta SINR > \Delta SINR_n(i)\big) \qquad i \in 1, \dots, N_{AMC} \tag{3.6}$$

This probability vector is used as in the previous methods to calculate the expected throughput for each possible CQI. Finally the CQI that maximizes equation 3.7 is fed back over the uplink channel.

$$T_{exp}(CQI_i) = efficiency(CQI_i) \cdot \sum_{cqi \geq CQI_k} \hat{p}_n(cqi) \qquad i \in 1, \dots, N_{AMC} \tag{3.7}$$

3.1.5 Methods comparison and adaptation to different velocity

In Figure 3-4 a comparison between the results obtained simulating the methods presented in this chapter is shown. The simulation parameters applied are written in table 2-5.

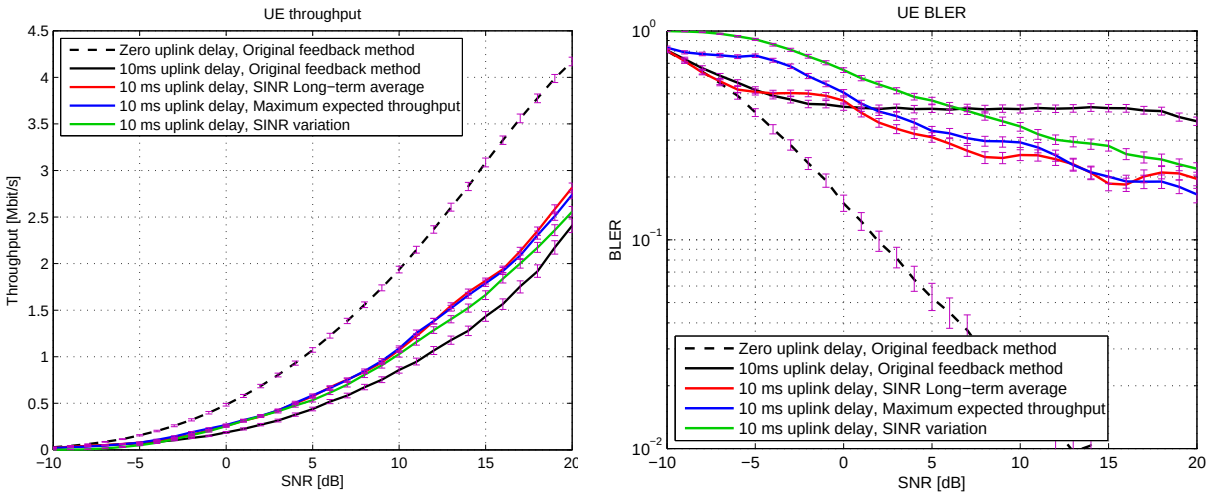

Figure 3-4 Throughput improvement methods comparison

The throughput results using the SINR Long term average method and Maximum expected throughput method are very similar, achieving an important improvement. With the SINR variation method there is also throughput improvement, nevertheless, not as large as with the previous ones. This happens due to the fact that the *t location-scale distribution* function does not fit the SINR variation sufficiently proper, and the probability vectors obtained are not accurate enough.

With regard to the BLER, the lower values are reached using the SINR long-term average method, which even improves the results obtained with the original method in most of the SNR points. In the other two cases there is only BLER improvement at high SNR.

METHODS EVALUATION OVER NORMALIZED DOPPELR FREQUENCY

In order to know the range of velocities and uplink delays where the methods explained before can work properly, some comparisons are simulated over normalized Doppler frequency. The simulation parameters are written in table 2-6. Figure 3-5 shows the results when the uplink delay is fixed to 1 ms, beta is fixed to 10 and the velocity varies from 0 to 300km/h.

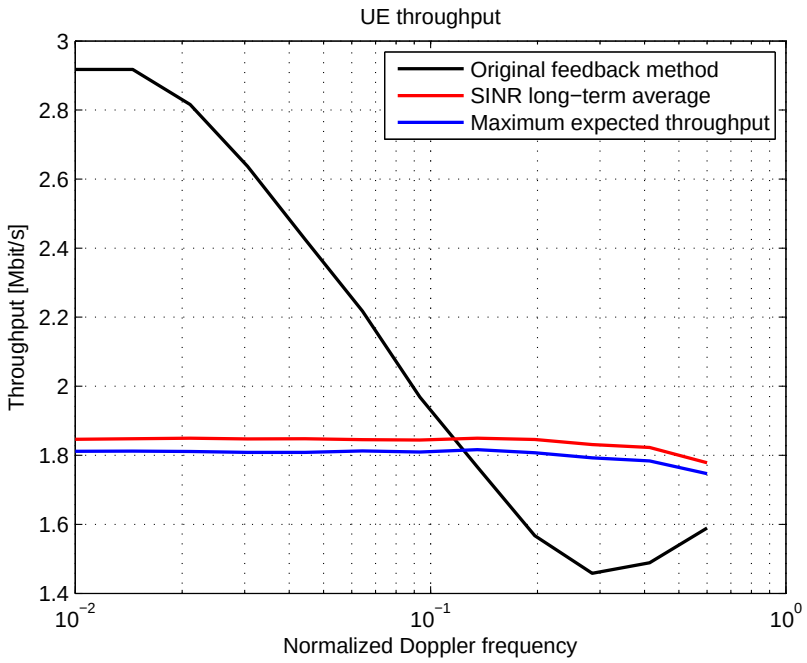

Figure 3-5 SISO Throughput over normalized Doppler Frequency and beta = 10

When the velocity is not severely high (up to 0.1 Normalized Doppler that corresponds to ≈50 km/h with the simulation parameters used), the temporal channel correlation is strong and it is not necessary to estimate an average of the SINR and the CQI, the original feedback method works properly.

The expressions used to average the SINR and the CQI in the SINR long-term average and Maximum throughput expected methods depend on the parameter β (equation 3.1 y 3.3). This parameter β defines the weight factors applied to the instantaneous and the previous averaged channel characteristics and can be adapted depending on the normalized Doppler frequency. Through simulations of these methods applying different beta parameter has been concluded that up to 0.1 normalized Doppler frequency the highest performance is achieved by setting beta equal to 1, which means no average. On the contrary, from 0.1 normalized Doppler frequency the temporal channel correlation decreases substantially fast and the best performance is achieved using a larger beta value. The most appropriate beta is equal to 10 because it achieves higher throughput than with lower beta values, nevertheless not higher than with larger values.

$$\beta = \begin{cases} 1 & si \quad \bar{f}_d \leq 0.1 \\ 10 & si \quad \bar{f}_d > 0.1 \end{cases} \tag{3.8}$$

The last investigation in this chapter is a comparison between the adapted methods and a linear predictor. The linear predictor basically calculates a linear interpolation of the previous channel realizations that are stored in a predictor buffer. Then an

extrapolation of these data gives a prediction of the current channel, therefore temporal correlation between consecutive subframes is essential.

Figure 3-6 shows how the throughput achieved using the methods implemented in this chapter behave similarly to the original feedback method at low velocity (when beta equal to one is used). It is above 0.1 normalized Doppler frequency when there is throughput improvement due to the averaging filters (applying a beta value equal to 10).

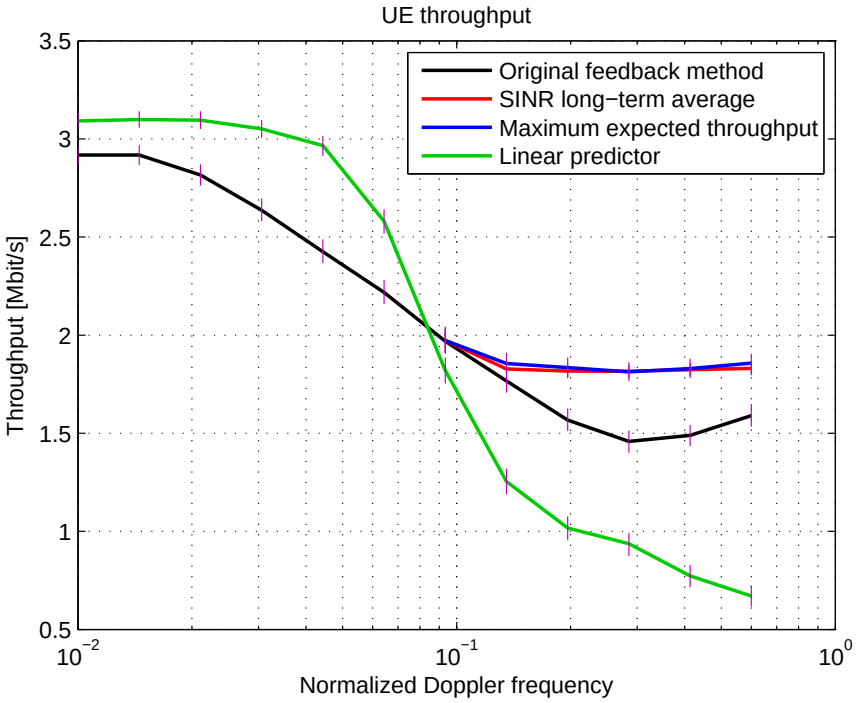

Figure 3-6 Throughput comparison with a linear predictor

The linear predictor gives throughput gain at low-median normalized Doppler frequency and above 0.1 the performance decreases rapidly. This is because the temporal channel correlation becomes weaker when the velocity increases and the linear predictor does not work anymore.

With regard to the BLER, (Figure 3-7) the predictor achieves excessive values at high speed while with the new implemented methods the BLER is lower even than with the original method, whose maximum is 40%. Specifically, using the maximum expected throughput method the BLER saturates at 31% and using the SINR long-term average the BLER saturates at 18%, which are very important improvements.

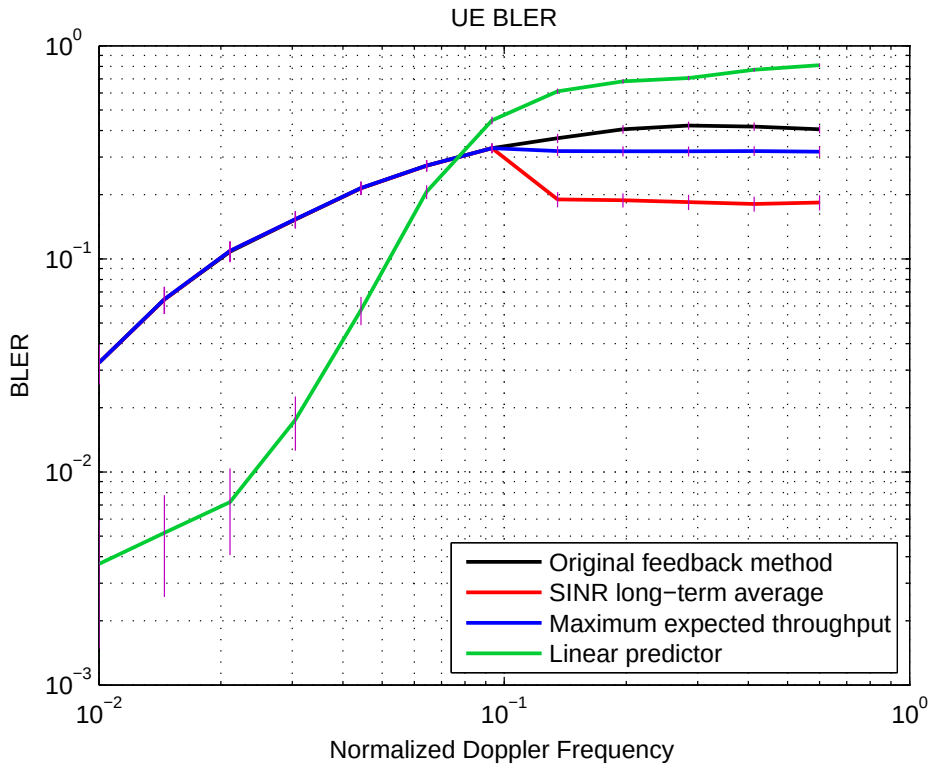

Figure 3-7 BLER comparison with a linear predictor

The utilized method should depend on the normalized Doppler frequency, selecting the linear predictor up to 0.1 and the SNR Long-Term Average or the Maximum throughput expected method above that value.

3.2 Study of the RI and PMI

In this section the proposed adapted methods are evaluated by using MIMO antenna configurations. As explained in the theory, when multiple antennas are used in the transmitter and the receiver a pre-transmission spatial preprocessing of the data is necessary because several spatial streams are formed. The spatial preprocessing at the eNodeB depends on the rank indicator and the precoding matrix indicator that are calculated in the receiver.

The modifications that are applied to the original feedback method are explained below.

3.2.1 CSLM Code modifications

- ***CQI selection***: When there are multiple antennas in the transmitter and in the receiver the CQI adaption method should be calculated separately for each layer, applying different SINR long-term averaging filters. However, this does not increase significantly the computational cost with respect to the original feedback algorithm.

- ***PMI selection***: In the original code this indicator is calculated by maximization of the post-equalization mutual information for each subband, as explained in section 2.2.4. The mutual information can be seen as a measure of the instantaneous channel capacity, whose estimation depends on the SINR. In turn, the SINR estimation depends on the precoding matrix used at each realization.
  Due to the high velocity that means a short channel coherence time and the large uplink delay, the post-equalization mutual information is not an accurate measure. This is because the PMI calculated at each time instant could not be optimum at the moment of its aplication. The best option is to fix a specific indicator and to use always the same precoding matrix in case the feedback delay is large compared to the channel coherence time.

- ***RI selection:*** In the legacy feedback algorithms a first approximation of the rank indicator $\hat{V}$ is obtained by maximization of the post-equalization mutual information with respect to the possible ranks. Nevertheless, the final indicator is selected between $\hat{V}$ and $\hat{V}-1$ by maximization of the sum efficiency.
  In the type of scenarios where the simulations are performed, the mutual information is not an appropriate measure, as explained above, so it is not estimated. Instead of the mutual information, the sum efficiency over layers for every possible rank is calculated and maximized, obtaining a first approximation of $\hat{V}$. This RI value tends to fluctuate over consecutive realizations, once again due to the channel variations, and the maximum throughput is not always achieved. In order to smooth these fluctuations a simple algorithm is implemented. It basically consists of storing in a vector the last k RI values calculated by the algorithm, selecting as the final RI the majority of the stored values.

3.2.2 Results

The first configuration studied is the one with the minimum number of antennas in the transmitter and the receiver, but more than one layer, which is 2x2 Single User MIMO (two antennas in both transmitter and receiver). The rest of the simulation parameters utilized are written in table 2-7. An important goal of the design in MIMO is that the different antennas should not be spatially correlated in order to exploit the diversity. The performance obtained with the original feedback method and without antenna correlation is represented in Figure 3-8.

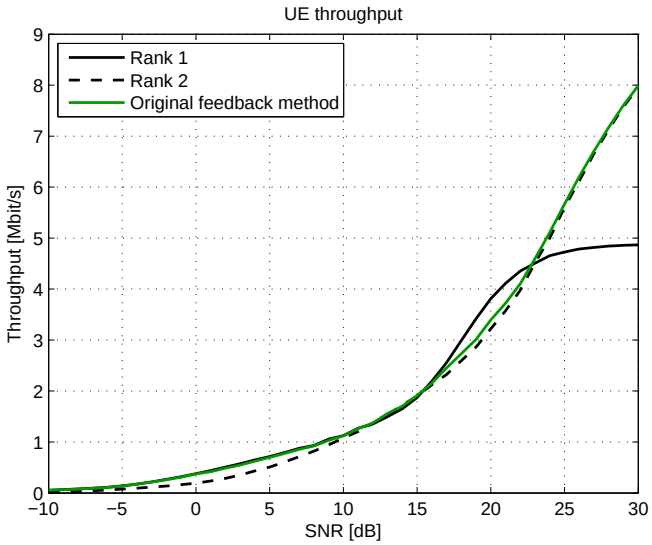

Figure 3-8 2x2 MIMO, Zero antenna correlation

It can be seen that the throughput achieved at low SNR is very similar for rank 1 and rank 2. In order to investigate about RI selection, 0.5 receiver antenna correlation is introduced to make this RI decision more difficult for the algorithm. In Figure 3-9 it is shown how the gap between rank 1 and 2 increases when 0.5 receiver antenna correlation is applied. This happens because the spatial correlation correlates the signals received over the received antennas, which basically implies that the largest singular value of the channel matrix grows, while the other singular values become smaller. As a result we obtain an increased SNR gap between rank 1 and the rest of the transmission ranks.

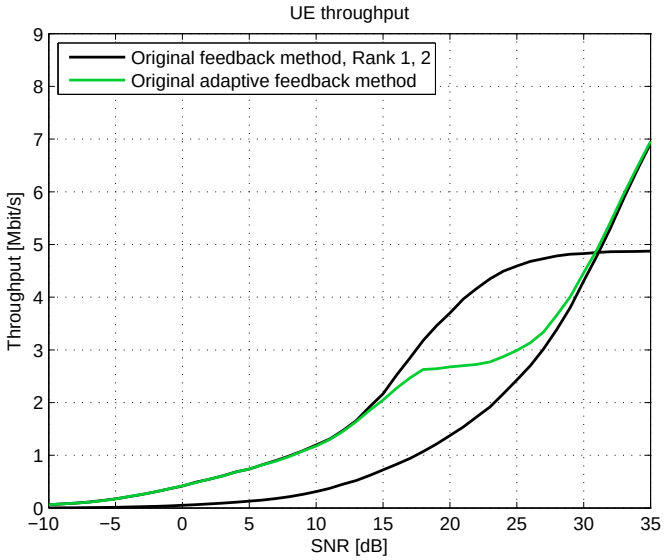

Figure 3-9 2x2 SU-MIMO throughput with 0.5 receiver antenna correlation

Now, with receiver correlation, is possible to observe how the CQI feedback method works properly when the performance is calculated for each rank separately, however, when the original RI adaptation is applied (green line) the performance decreases significantly between 15 and 30 dB because the algorithm does not select the optimum RI because of its fluctuations over time.

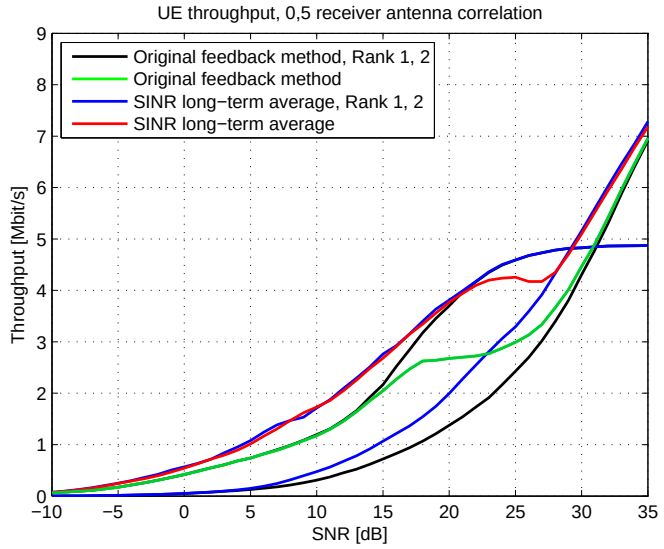

Figure 3-10 2x2 SU-MIMO throughput improvement with 0.5 antenna correlation

In Figure 3-10 the SINR long-term average method is applied firstly to each layer separately, obtaining the results represented by blue lines. Then the algorithm for RI adaptation that estimates the majority of the previous values selected is applied, obtaining the throughput represented by the red line. Although the RI majority is used, between 20 and 30 dB the number of times that the original method selects rank one and rank two is about 50%, as a result, even the majority value fluctuates in that SNR

range. There is improvement with respect to the original results; however, the proposed methods are still not optimum with this antenna configuration. Then a more complex configuration with 4 transmit antennas and 8 receive antennas is used to simulate the same comparison as before. The results are depicted in Figure 3-11.

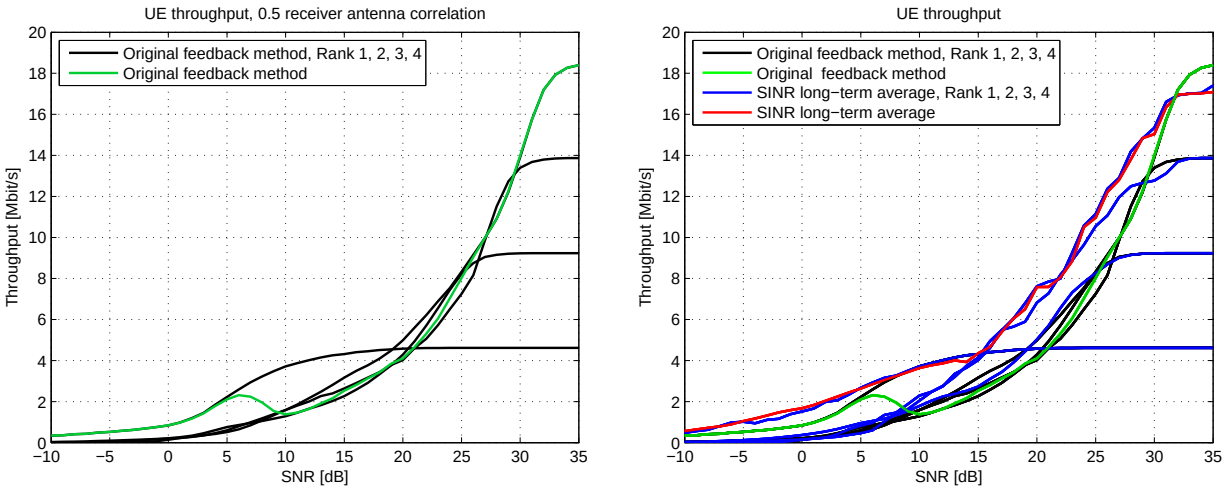

Figure 3-11 4x8 SU-MIMO throughput with 0.5 receiver antenna correlation and throughput improvement

In the figure on the left it can be observed that the original RI adaptation does not work. In the figure on the right (green), applying this antenna configuration the majority algorithm works perfectly (red), achieving the maximum throughput at any SNR value.

Finally a comparison between the results obtained with the new feedback method and the original feedback method with zero uplink delay (that corresponds to the maximum theoretical throughput with the parameters used) and 10ms uplink delay is simulated. The results are depicted in Figures 3-12 and 3-13.

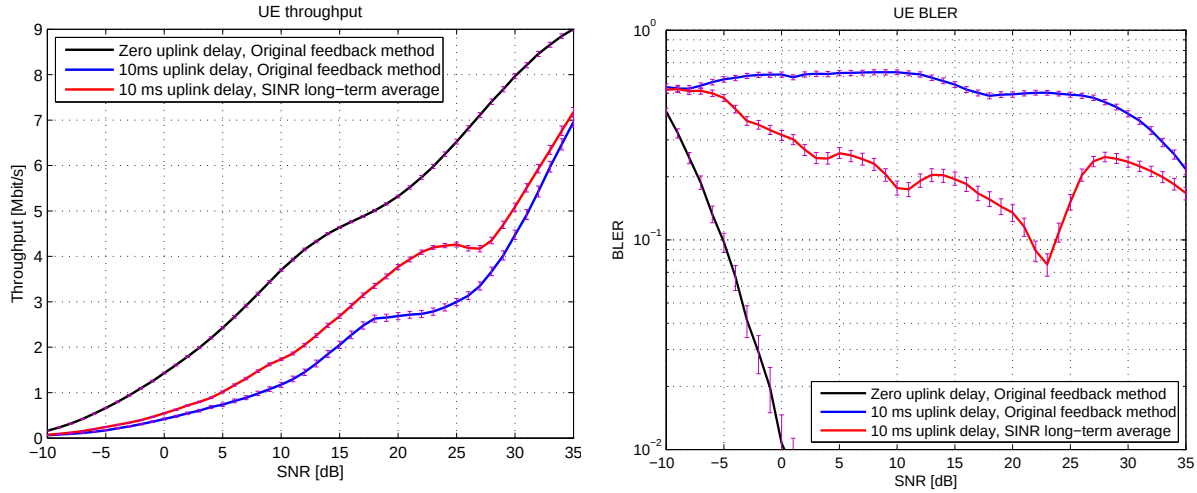

Figure 3-12 2x2 SU-MIMO throughput comparisons with the original feedback method

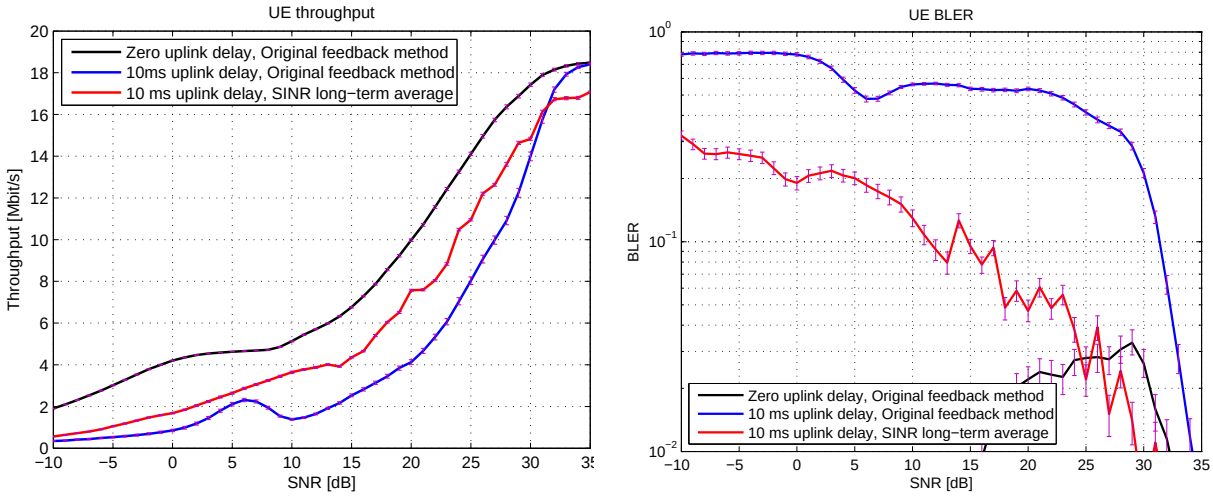

Figure 3-13 4x8 SU-MIMO throughput comparisons with the original feedback method

The figures on the left show throughput improvement with respect to the results obtained using the original feedback method with 10 ms uplink delay when the SINR long-term average method is simulated. Furthermore, BLER improvement can also be observed in the figures on the right. These improvements increase with the use of more complex antenna configurations.

3.3 Frequency-selective channel with multiple users

During the work presented up to now, where a flat fading channel and only one user have been simulated, the calculation of the CQI and PMI have been wideband, i.e., an average of the channel characteristics over the whole bandwidth has been estimated and the same indicator values have been reported over all RBs.

In this section the performance obtained when simulating a time and frequency selective channel with multiple users is studied. In section 2.2.4 the feedback indicators calculation is detailed. It is possible to estimate either wideband or subband CQI and PMI indicators, depending on the CQI and PMI granularity configured in the simulator. An average CQI/ PMI over the whole available bandwidth is estimated in case the granularity is set to six. On the other hand, different CQI and/or PMI are estimated for each subband when the granularity is configured to one. Considering that the total bandwidth used in the simulations is 1.4 MHz and the subcarrier spacing selected is 15 kHz, the bandwidth assigned to each RB is 180 KHz, being also this value the minimum subband bandwidth. In this study the four possible combinations of CQI

and PMI granularities six and one are simulated. The simulation parameters are available in table 2-8, moreover, four transmitter antennas and two receiver antennas are used.

The scheduling strategy used in this section that allows assigning the physical resources to the users is *Maximum Rate.* The goal of this strategy is to maximize the system throughput taking the scheduling decisions according to the reported channel quality. It tries to transmit to users with favorable radio-link conditions, which allows obtaining multi-user-diversity gain.

The solid lines in Figure 3-14 represent the cell throughput obtained using the original feedback method. At low $\overline{f_d}$ the highest performance is achieved with CQI and PMI granularity one due to the high temporal channel correlation. Above 0.1 $\overline{f_d}$ the performance decrease rapidly and it is from this point where the new feedback method implemented that calculates an SINR average achieves the highest performance.

In order to study the range of normalized Doppler frequency where the PMI adaptation obtains throughput improvement using the SINR long-term average method, the PMI feedback has been activated during the simulations in this section. The lines with circles represent the results of setting the four possible PMI and CQI granularity combinations of one and six and using the SINR long-term average method.

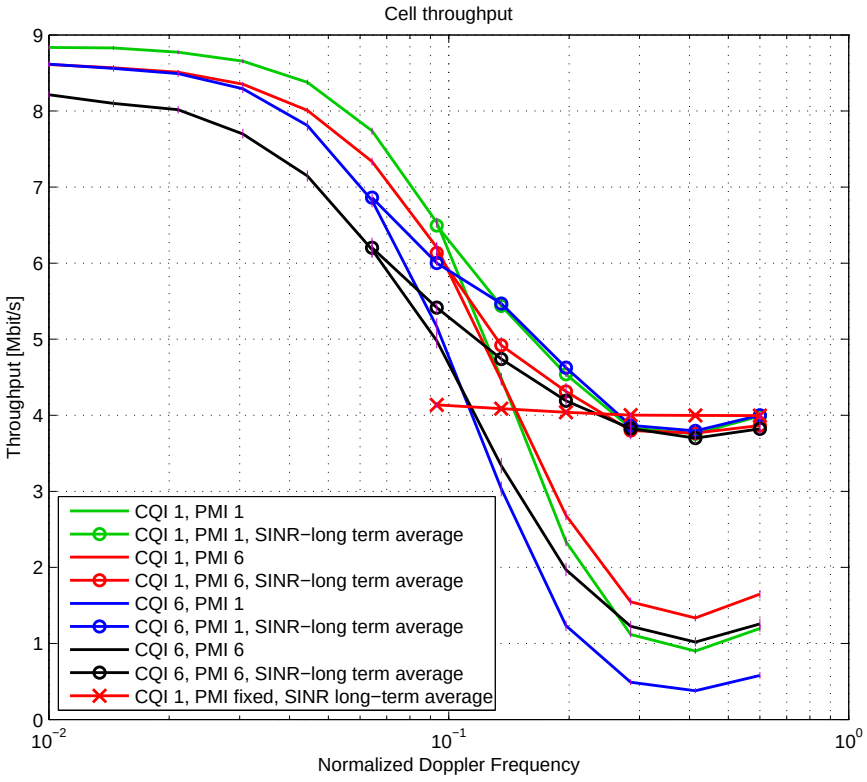

Figure 3-14 Cell throughput improvement using SINR long-term average method

From $\overline{f_d}$ equal to 0.1 up to 0.3 the highest performance using the new feedback method is still achieved with PMI granularity one, however, from 0.3 $\overline{f_d}$ it can be seen how the results are very similar irrespective of the indicators granularity. This behaviour is due to the fact that the channel variations become extremely fast and the SINR average over consecutive RBs stays practically flat. The same occurs with the BLER results, which are shown in Figure 3-15.

Finally the SINR long term average method has been simulated from 0.1 $\overline{f_d}$ with CQI granularity equal to one and fixed PMI. The result corresponds to the red line with crosses. In Figure 3-14 it can be observed that from around 0.3 $\overline{f_d}$ the throughput achieved is even higher than using the original feedback method. Nevetheless, this is not the only improvement, for the same $\overline{f_d}$ range the BLER decreases considerably, from 40% with adaptive PMI to 26% with fixed PMI, as depicted in 3-15.

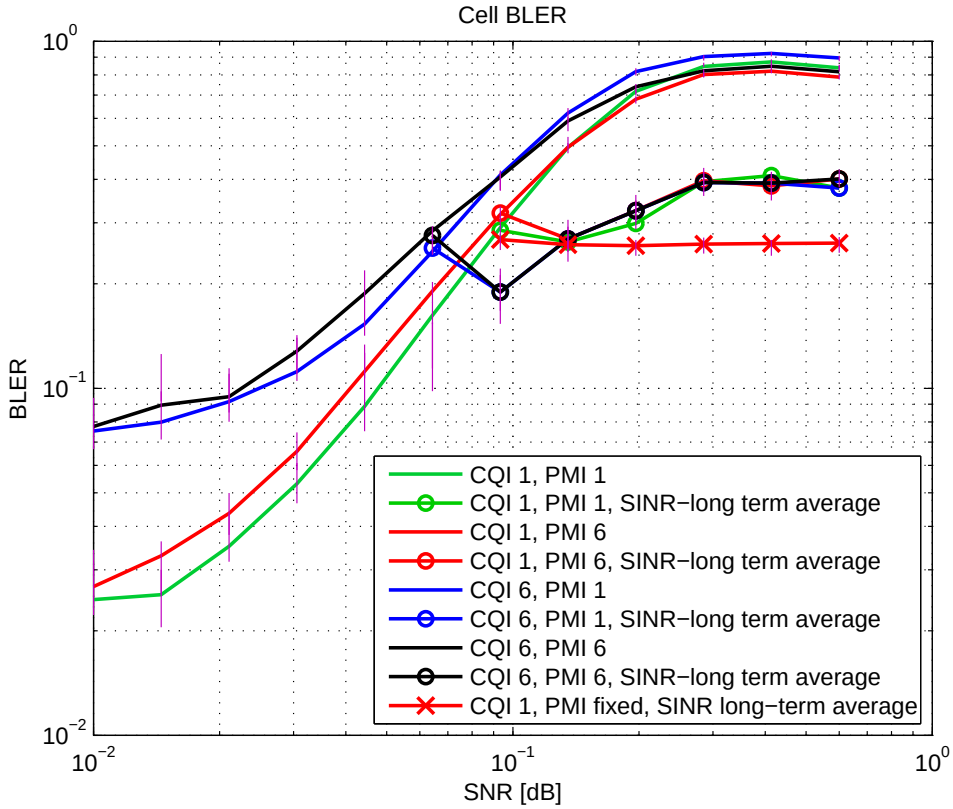

Figure 3-15 Cell BLER improvement using SINR long-term average method

4. FEEDBACK ALGORITHMS TO ACHIEVE THE 0.1 BLER TARGET

This chapter presents the new algorithms designed to fulfil the 0.1 BLER target at the first HARQ transmission. In addition to accomplish the BLER target, the methods also try to achieve the maximum throughput.

4.1 Study of the CQI

4.1.1 0.1 BLER target method

This method achieves the 0.1 BLER target by exploiting exclusively the instantaneous channel knowledge. For that purpose a new SINR to CQI mapping table needs to be created.

It has been already explained in section 2.2.3 that the SINR-to-CQI mapping table is obtained by simulating the BLER performance for all CQI values. The SINR values in the table are equal to the AWGN SNRs at 10 % BLER. Once the SINR is estimated at the receiver, it is compared to the SINR values in the tables and the maximum CQI that allows transmission without exceeding 10 % BLER is selected.

With the purpose of creating a new mapping table to achieve the target, the BLER curves for each CQI have been simulated with the feedback deactivated and in a scenario with zero channel correlation and 10ms uplink delay. These curves are represented in Figure 4-1 and show how the BLER decreases when the SNR increases. Then the new mapping table is created with the SNR points at 0.1 BLER at each BLER curve.

This method has two disadvantages:

1. The new mapping table is optimized for a channel model with zero temporal correlation and 10ms uplink delay, which can be considered as the worst possible scenario. This means that using the new mapping table the BLER target is achieved simulating any other scenario, however, the performance will not be optimum.

2. In chapter 2 has been explained that due to the correlation and uplink delay parameters used it is not appropriate to take into account exclusively instantaneous channel conditions because the CQI estimated is not optimum at the moment of its application.

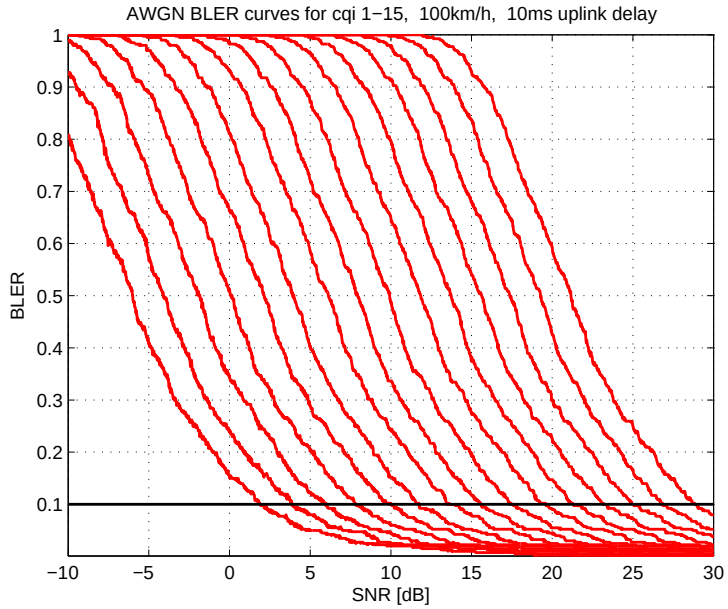

Figure 4-1 BLER curves for CQI 1-15 with zero correlation and 10ms uplink delay

4.1.2 Expected BLER method

The goal of this algorithm is once again to maintain the BLER values below 10% and at the same time to solve the drawbacks that the previous method presents. By using this method, the 0.1 BLER target is achieved with any correlation and uplink delay parameters, besides, it also tries to achieve the highest throughput by taking advantage of the channel statistics.

The method involves estimating the expected BLER for each possible modulation and coding scheme, selecting the highest CQI that achieves the target. The AWGN SNR-BLER curves obtained with optimum channel conditions (high temporal correlation and zero uplink delay) are employed for that purpose. These curves are depicted in Figure 4-2.

The first step consists of storing in a vector the instantaneous SINR values obtained during the last k realizations.

$$t_n = [SINR_n, SINR_{n-1}, SINR_{n-2}, \dots, SINR_{n-k}] \tag{4.1}$$

Once these values are known, all of them are evaluated over each BLER curve separately, calculating an average and obtaining the BLER expected result for each possible CQI.

$$BLERexp(CQI_i) = \frac{1}{longitud(t_n)} \sum_{j=0}^{k} BLER_{CQI_i}(SNR_{n-j}) \tag{4.2}$$

In equation 4.2 $BLER_{CQI_i}$ represents the specific BLER curve obtained with CQI "i". Finally the CQI with highest BLER expected below 0.1 is selected.

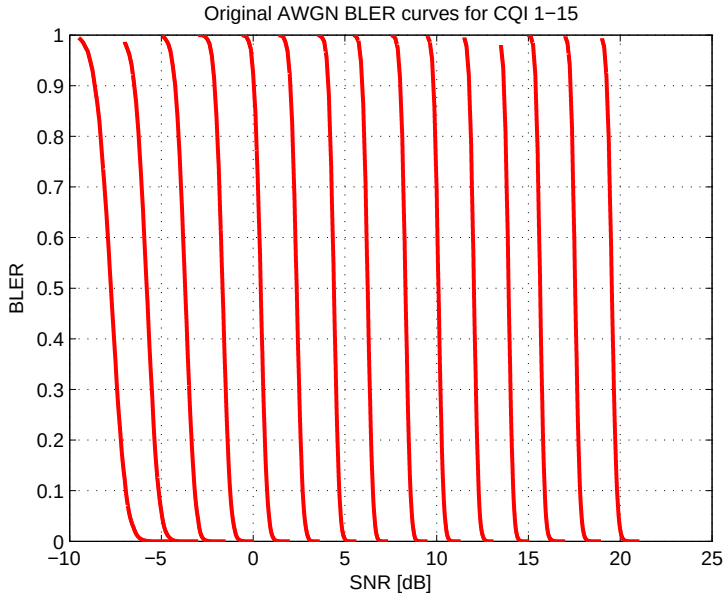

Figure 4-2 BLER curves for CQI 1-15 with maximum correlation and zero uplink del

4.1.3 Methods comparison and evaluation over normalized Doppler frequency

Figure 4-3 represents a comparison between the results obtained applying the original feedback method and the previous methods explained in this chapter that achieve the BLER target. The simulation parameters are available in table 2-5.

The figure on the right represents the BLER in the receiver. The results show a BLER remaining below 0.1 when the new methods implemented are used; however, in the figure on the left it is shown that the throughput has decreased, especially when using the 0.1 BLER target method that only exploits the instantaneous SINR values.

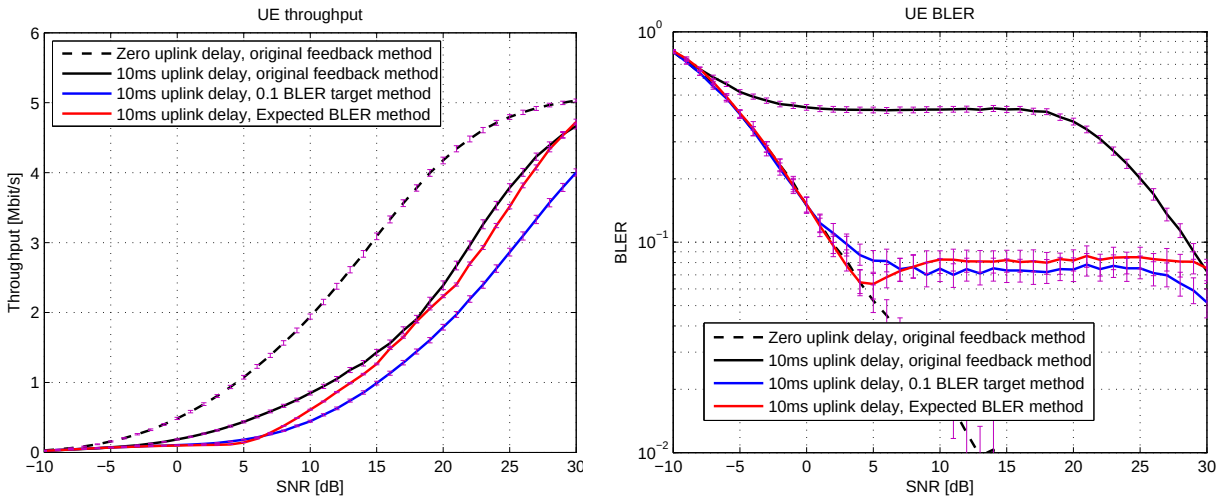

Figure 4-3 Methods comparison that achieve the 10% BLER

Afterwards, the methods are evaluated over the normalized Doppler frequency applying the simulation parameters in table 2-6. It is shown on the right of Figure 4-4 that with the BLER expected method the BLER target is fulfilled at any $\overline{f_d}$ while improving the throughput with respect to the 0.1 BLER target method. On the contrary with the original method the BLER increases with the velocity, up to 0.4, a considerable high value.

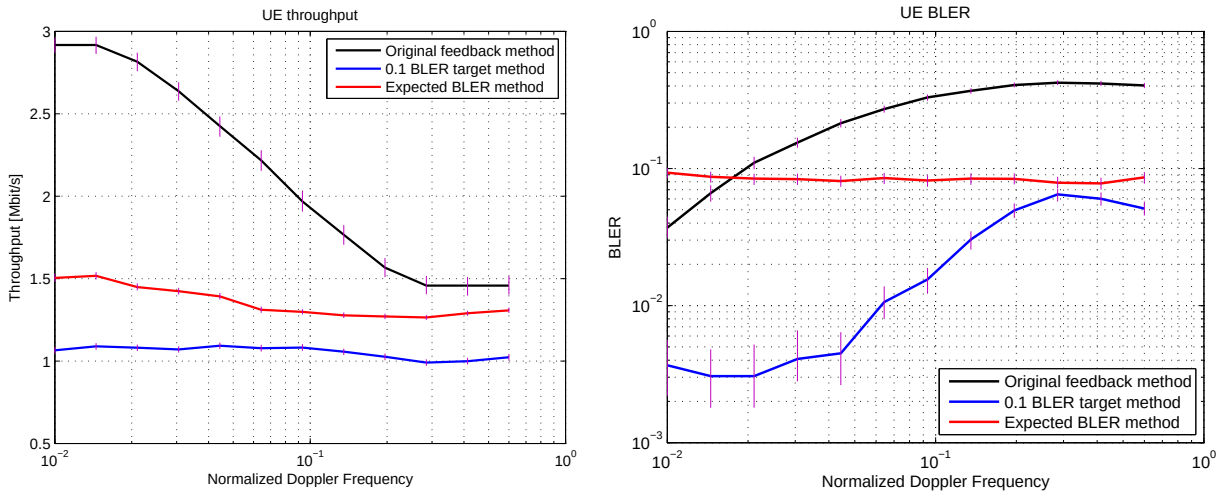

Figure 4-4 Methods comparison that achieve 10% BLER over $\overline{f_d}$

The algorithm that better performance offers is the BLER expected method because it achieves the highest throughput while the BLER values remain below the target. For that reason this is the method selected to be applied when more complex antenna configurations are used in the following section.

4.2 Study of the RI and PMI

As in the previous chapter the PMI and RI feedback values are studied over antenna configurations that require spatial preprocessing. The simulation parameters used in this section can be consulted in table 2-7. In this case, the results obtained using the BLER expected method are compared with the results obtained using the 0.1 BLER target method. The purpose of this comparison is to observe the improvement that can be obtained when the channel statistics are exploited.

4.2.1 CLSM Code modifications

The algorithms employed to calculate the PMI and RI are similar than the studied in the previous chapter, that is, the PMI value is fixed and the optimum rank indicator is calculated by maximization of the sum efficiency over layers (calculated for every possible rank) and finally the majority of the previous values selected by the algorithm is chosen.

4.2.2 Results

The first antenna configuration evaluated is once again 2x2 MIMO with one user.

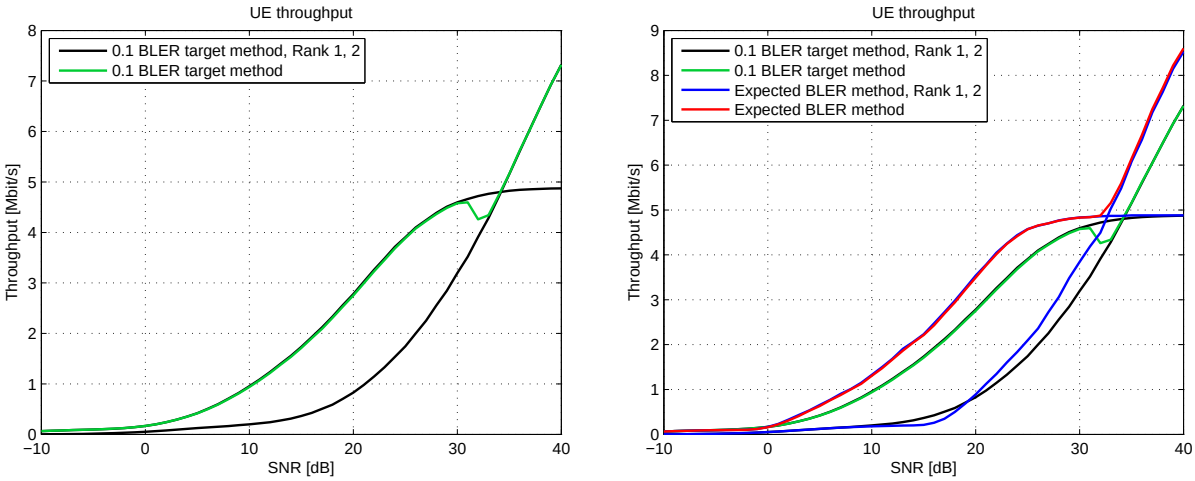

Figure 4-5 2x2 MIMO, throughput improvement achieved using the BLER expected method

In Figure 4-5 the results obtained with two transmitter antennas and two receiver antennas are shown. On the left it can be seen that with the 0.1 BLER target method the original RI adaptation does not achieve the maximum throughput between 30 and 35dB SNR (green line). On the contrary, in the figure on the right the majority of the previous RI selected has been applied together with the BLER expected method (red line), achieving the maximum performance at any SNR value.

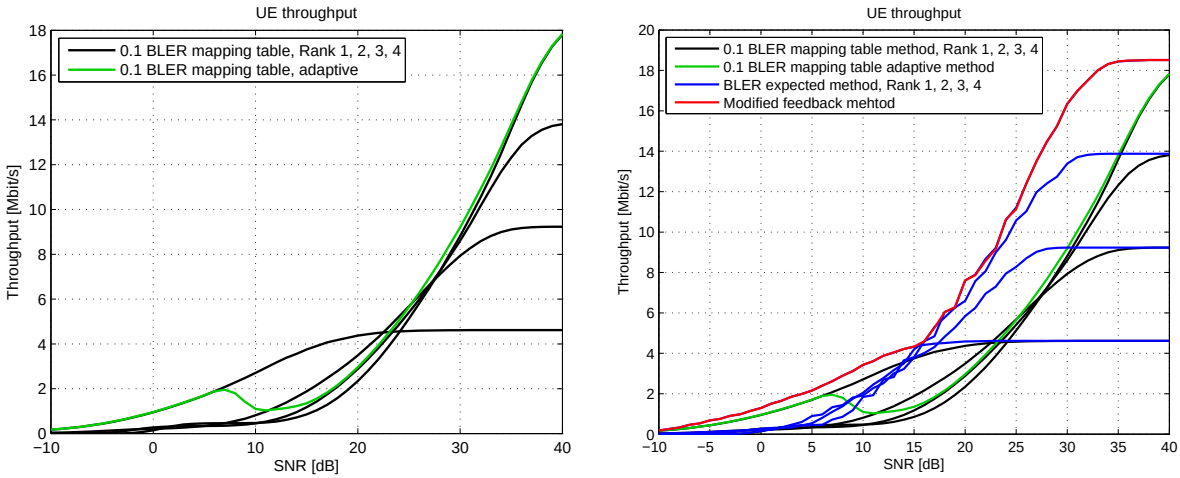

Figure 4-6 4x8 MIMO, throughput improvement achieved using the BLER expected method

The same comparison is simulated and represented in Figure 4-6 using 4x8 MIMO antenna configuration. With the same notation than before, it can be observed on the left that the original algorithm for RI adaptation does not work properly and in the figure on the right that the maximum performance is achieved using the BLER expected method and calculating the majority of the previous RI selected (red line).

Lastly, in the following figures the final results with the two methods that achieve the BLER target are compared to the results using the original feedback method with zero uplink delay.

In figure 4-7 on the right it can be seen that with 2x2 antennas the BLER target is achieved at SNR values above -5dB while in Figure 4-8 with 4x8 antennas the BLER target is achieved at any SNR point. Regarding to the throughput results, as in the previous chapter, the more complex antenna configuration is employed, the more throughput improvement is achieved.

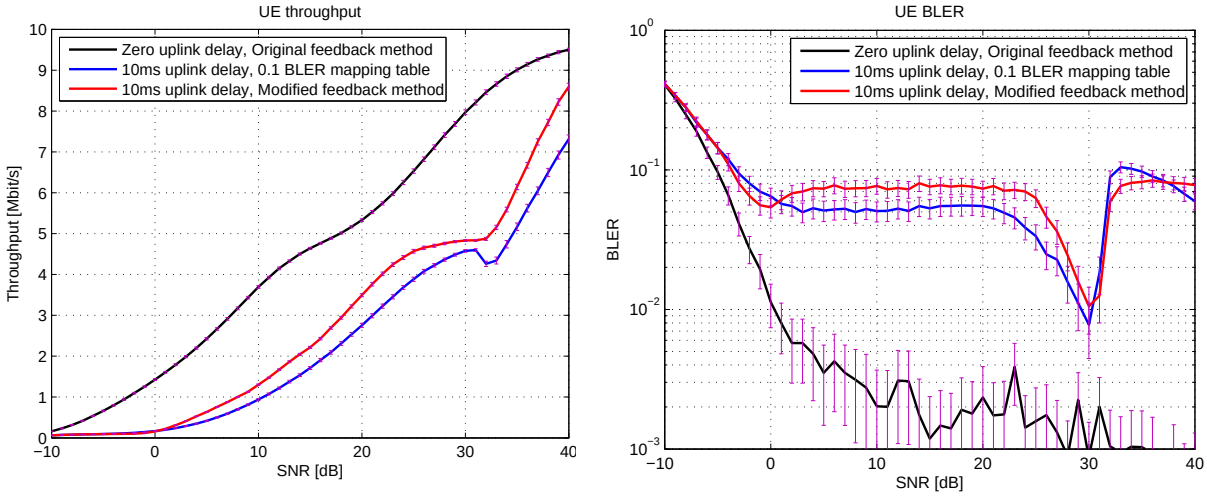

Figure 4-7 2x2 MIMO, final results that achieve the BLER target

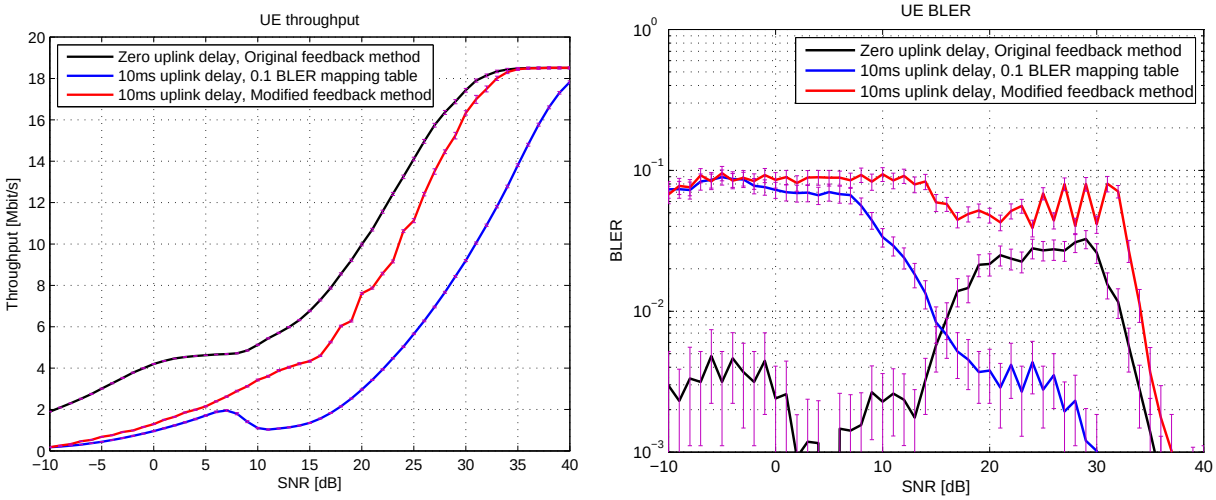

Figure 4-8 4x8 MIMO, Final results that achieve the BLER target

4.3 Frequency-selective channel with multiple users

In this section the last investigation is explained. With the aim of studying the performance obtained using the new feedback algorithms when several users are placed in the same scenario, a frequency-selective channel with the simulations parameters in table 2-8 is applied. In addition to these parameters, different combinations of CQI and PMI granularity are simulated, specifically the four possible combinations of granularity one and six.

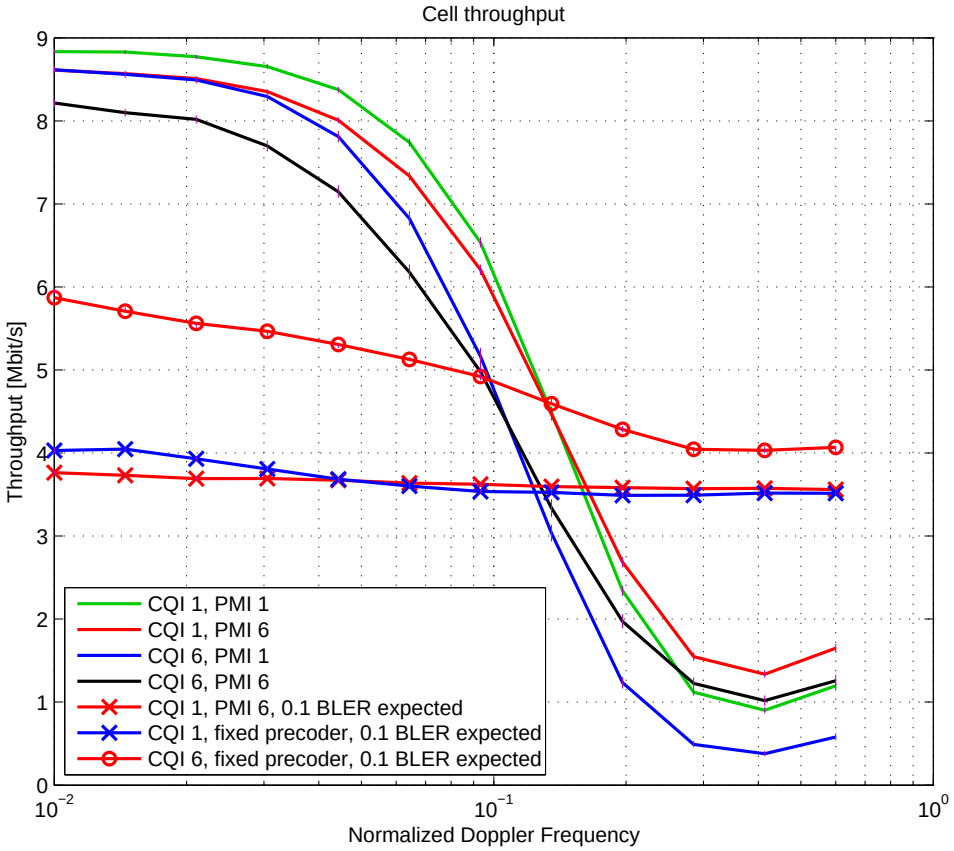

Figure 4-9 Cell throughput improvement with BLER expected method

The solid lines in Figure 4-9 represent the results obtained with the four different granularity configurations and using the original feedback method. When the normalized Doppler frequency is below 0.1 the highest performance is achieved by estimating a different CQI and PMI for each subband because the temporal correlation is profound and the channel coherence time is not severe. Nevertheless, when the normalized Doppler frequency increases above 0.1 the highest performance is obtained by estimating a common PMI for all the available RBs because the correlation decreases.

The red line with circles represents the result of applying again the BLER expected method with CQI granularity one but in this case with adaptative PMI (granularity six). The throughput obtained is higher than with fixed PMI, however, it can be seen in Figure 4-10 that the BLER target is not achieved above 0.1 normalized Doppler frequency. This happens because the PMI selected has been calculated under specific channel conditions that have changed in the moment it is applied.

Finally, the red and blue lines with crosses correspond to the results obtained using the BLER expected method with CQI granularity one and six, respectively, and both with fixed PMI. These results are very similar in terms of throughput (Figure 4-9). With regard to the BLER (Figure 4-10), when the CQI granularity is six the BLER values are

close to 0.1, however, above this point. This is because an average CQI has been estimated over all the RBs, which are assigned to different users, therefore if some user is exposed to worst channel conditions it will not achieve the target with the CQI estimated by averaging the channel conditions. The BLER target is only achieved at any normalized Doppler frequency with CQI granularity one and fixed PMI.

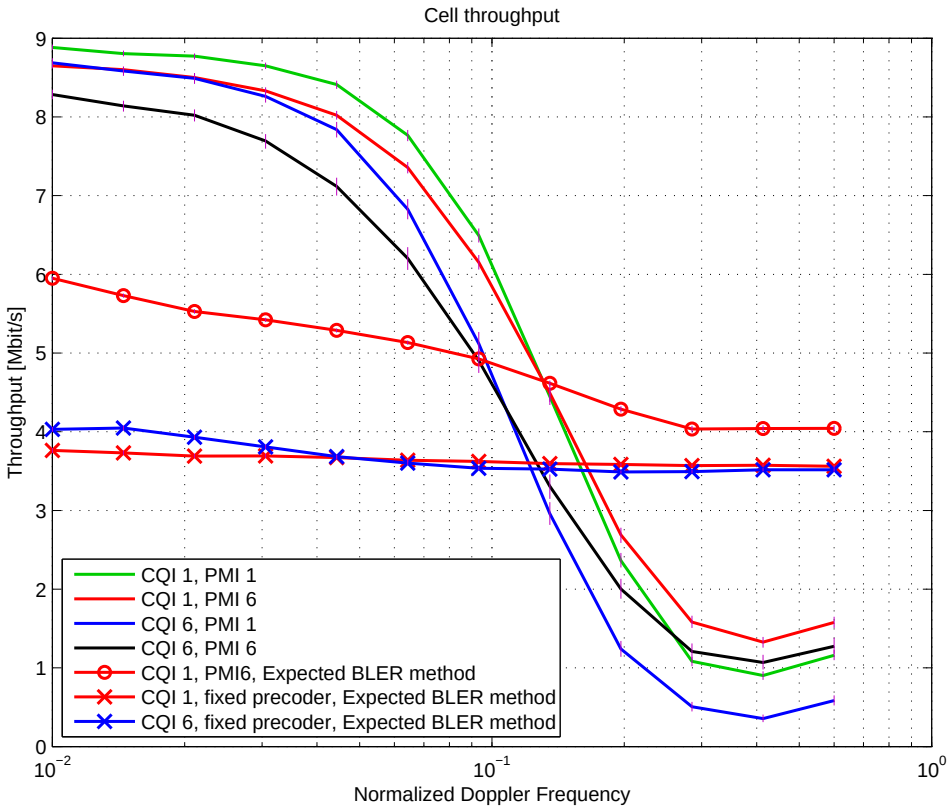

Figure 4-10 Cell BLER improvement with BLER expected method

5. CONCLUSIONS AND FUTURE RESEARCH

During the development of this thesis has been proved by simulations in different scenarios that the user performance in terms of throughput and BLER decrease considerably with the user velocity.

The two objectives considered at the beginning of these report are satisfied through the implementation of new feedback algorithms that consider the channel statistics to calculate the feedback indicators. The first objective is the improvement of the throughput obtained by the user without considering that the BLER values are above 10% in most of the cases, and the second objective is the compliance of BLER results without exceeding 10% due to this is the highest working point recommended in wireless communications.

When it comes to interpreting the results presented, the fact that the HARQ process could not be applied should be taken into account. In practice, it is expected a BLER target fulfilment.

Regarding the study of the CQI, during which a SISO antenna configuration has been employed, it can be concluded:

- The methods designed to improve the throughput achieve an important improvement from 0.1 normalized Doppler frequency (corresponds to 50km/h with 1ms uplink delay and 2.1GHz frequency carrier). In addition, the BLER results are substantially lower compared to the BLER results using the original algorithm, nevertheless above 10%.

- The BLER expected method achieves BLER<0.1 at any normalized Doppler frequency point, however, this method implies a loss in throughput compared to the results using the original feedback method.

With respect to the RI and PMI investigation, during which a MIMO antenna configuration has been utilized, the main conclusions are:

- An increased throughput improvement and a decreased BLER values have been observed when using more and more complex antenna configurations.

- In channels with considerably weak temporal correlation a fixed PMI offers better results.

Lastly, through evaluating the proposed methods in a time and frequency selective channel with multiple users it has been proved that:

- Once again the performance using the methods developed to improve the throughput achieve gain with respect to the original feedback method when the normalized frequency Doppler is above 0.1, reaching the same throughput and BLER values irrespective of the CQI and PMI granularity with normalized Doppler frequency above 0.25.

- The BLER expected method achieves the BLER target exclusively with CQI granularity equal to one (different CQI value calculate for each RB/user) and a fixed PMI value.

Even though the simulations have been performed using different antenna configurations, different channel models and other different simulation parameters, future research that could give us interesting results can be performed,

1. Results validation by applying the HARQ process. The 10% BLER boundary should be accomplished with all the methods proposed and in any simulated scenario.

2. Transmission mode 3 (OSLM) application, which is the most widely used at very high velocity. This transmission mode is explained in section 2.2.2. Basically it does not rely on any precoding matrix recommended by the user, using a fixed precoding matrix defined by the standard. Furthermore, the diversity is increased by incorporating Cyclic Delay Diversity.

3. Simulation of a non-perfect channel estimation. With the implementation of a different channel estimation that introduces errors, the simulations would be more realistic and a performance loss with the velocity with respect to the results presented in this thesis would be observed.

4. Evaluation of the new feedback methods over MU-MIMO where the users are spatially multiplexed. An important improvement is not expected using this configuration because when the user velocity is considerably high the use of a higher number of antennas in the transmitted than in the receiver is recommended in order to obtain high user performance.

References

[1] JC Ikuno, C Mehlführer and M Rupp, “A novel link error prediction model for OFDM systems with HARQ” *Proc. IEEE International Conference on Communications (ICC 2011), Kyoto, Japan,* 2011

[2] Starsky H.Y. Wong, Hao Yang, Songwu Lu and Vaduvur Bharghavan, ”Robust Rate Adaptation for 802.11 Wireless Networks”, 2006

[3] Pravin Shankar, Tamer Nadeem, Justinian Rosca and Liviu Iftode “CARS: Context-Aware Rate Selection for Vehicular Networks”, IEEE 2008

[4] Technical Specification Group Radio Access Network, “E-UTRA; physical channels and modulation,” 3GPP, Tech. Rep. TS 36.211 Version 8.7.0, May 2009.

[5] S. Caban, C. Mehlführer, M. Rupp and M. Wrulich, “*Evaluation of HDSPA and LTE: From Testbed Measurements to System Level Performance*”, 2011.

[6] Stefan Schwarz, Christian Mehlführer and Markus Rupp, “Calculation of the Spatial Preprocessing and Link Adaption Feedback for 3GPP UMTS/LTE”, in *Proc. IEEE Wireless Advanced 2010*, London, UK, 2010.

[7] Stefan Schwarz and Markus Rupp, “Throughput maximizing feedback for MIMO OFDM based wireless communication systems”, in *Proc. Signal Processing Advances in Wireless Communications (SPAWC)*, 2011 San Francisco, CA.

[8] Erik Dahlman, Stefan Parkvall, and Johan Sköld “*4G LTE/LTE-Advancedfor Mobile Broadband*”, 2011

[9] Ramón Agusti, Francisco Bernardo, Fernando Casadevall, Ramon Ferrús, Jordi Pérez-Romero, Oriol Sallent, “*LTE: nuevas tendencias en comunicaciones móviles*”, 2010.

[10] M. J. Gans, “A power-spectral theory of propagation in the mobile-radio environment,” *IEEE Trans. Veh. Technol.,* vol. VT-21, pp. 27–38, Feb. 1972.

[11] R. H. Clarke, “A statistical theory of mobile-radio reception,” *Bell Syst. Tech. J.*, pp. 957–1000, Jul.–Aug. 1968.

[12] C. Mehlführer, J. C. Ikuno, M. Šimko, S. Schwarz, M. Wrulich, and M. Rupp, “The Vienna LTE simulators – Enabling Reproducibility in Wireless Communications Research”, *EURASIP Journal on Advances in Signal Processing*, 2011.

[13] S. Schwarz, J. C. Ikuno, M. Šimko, M. Taranetz, Qi Wang and M. Rupp, “Pushing the Limits of LTE: A Survey on Research Enhancing the Standard”, *IEEE Access*, 2013.

[14] Hassaan Touheed, Atta Ul Quddus and Rahim Tafazolli, “An Improved Link Adaptation Scheme for High Speed Downlink Packet Access”, *Vehicular Technology Conference, 2008*. VTC Spring 2008. IEEE, Singapore.

[15] S. Schwarz, M. Wrulich, and M. Rupp, “Mutual Information based Calculation of the Precoding Matrix Indicator for 3GPP UMTS/LTE”, in *Proc. IEEE Workshop on Smart Antennas 2010*, Bremen, Germany.

[16] Stefan Schwarz, Christian Mehlführer and Markus Rupp, “Throughput Maximizing Multiuser Scheduling with Adjustable Fairness”, *IEEE International Conference on Communications (ICC)*, 2011, Kyoto.

[17] http://www.4gamericas.org/index.cfm?fuseaction=page&sectionid=272. Última visita a la web, Noviembre de 2014.

[18] White Paper, “Architectural Considerations for Backhaul of 2G/3G and Long Term Evolution Networks”. Disponible en http://www.cisco.com/c/en/us/solutions/collateral/service-provider/mobile-internet/white_paper_c11-613002.html. Última visita a la web, Noviembre de 2014

[19] White paper, “Doppler Spread and Coherence Time”. Disponible en http://www.ni.com/white-paper/14911/en/. Última visita a la web, Noviembre de 2014.